Article

The Daylighting Optimization of Integrated Suspended Particle Devices Glazing in Different School Typologies

Abdelhakim Mesloub [1,*], Mohammed Mashary Alnaim [1], Ghazy Albaqawy [1], Khaled Elkhayat [1], Rim Hafnaoui [2], Aritra Ghosh [3] and Mohammed Salah Mayhoub [4]

[1] Department of Architectural Engineering, Ha'il University, Ha'il 2440, Saudi Arabia; mm.alnaim@uoh.edu.sa (M.M.A.); g.albaqawy@uoh.edu.sa (G.A.); k.elkhayat@uoh.edu.sa (K.E.)
[2] Faculty of Engineering and Built Environment, Universiti Sains Islam Malaysi (USIM), Bandar Baru Nilai 71800, Malaysia; archirimy@raudah.usim.edu.my
[3] Faculty of Environment, Science and Economy (ESE), Renewable Energy, Electric and Electronic Engineering, University of Exeter, Penryn TR10 9FE, UK; a.ghosh@exeter.ac.uk
[4] Architecture Department, Faculty of Engineering, Al-Azhar University, Nasr City Campus, Cairo 11371, Egypt; msm@azhar.edu.eg
* Correspondence: a.maslub@uoh.edu.sa

Abstract: The design of school building typologies, along with the use of advanced glazing systems such as suspended particle devices (SPD), is crucial for determining visual comfort for students. Recent research has focused on integrating SPD in architectural elements such as skylights, clerestories, and windows. In hot desert climates, minimizing window areas, employing shading mechanisms, and utilizing daylighting features such as courtyards and atriums are practical. This study explores the optimization of various architectural components in classroom designs, including Window Wall Ratios (WWR), Skylight Ratios (SR), floor levels, cardinal orientation, and SPD switching states. Using a detailed and comprehensive radiance simulation via Rhino-Grasshopper and Colibri 2.0, we conducted a thorough analysis and optimization of the SPD glazing system across different states on both annual and hourly bases. The results indicate that optimizing SPD transmittance states between 30–40%, maintaining WWRs from 20–40%, and incorporating a large skylight ratio significantly enhances the recommended work plane illuminance (WPI) and the uniformity index (Ui) of the tested typologies. This optimization improves glare control across various building typologies and provides a roadmap for architects aiming to design learning spaces that prioritize visual comfort and overall student well-being.

Keywords: visual comfort; atrium; courtyard; clerestory; hot climate

1. Introduction

Indoor environmental quality (IEQ) is a crucial aspect of school buildings as it affects students' and staff's health, comfort, and productivity [1–3]. According to recent statistics, poor IEQ in school buildings can lead to absenteeism, decreased academic performance, and increased healthcare costs [4–6]. The Environmental Protection Agency (EPA) found that students in schools with poor IEQ scores have lower percentages on standardized tests than those with good IEQ [7]. One major factor contributing to poor IEQ in schools is visual comfort problems. These problems include poor daylighting, discomfort, and glare [8,9]. Poor daylighting can cause eye strain, headaches, and fatigue, decreasing productivity and absenteeism. On the other hand, glare can cause visual discomfort and make it difficult for students to see their work [10,11].

Despite energy-efficient and advanced lighting systems developments, daylighting is still a valuable architectural design element [12]. However, a conflict may arise between increasing window area for better daylighting and avoiding excessive glazing to reduce energy demand for heating or cooling [13]. This conflict can be resolved by selecting an

appropriate window-to-wall ratio (WWR) and considering other variables that affect heat transfer through windows, such as window orientation, room dimension, and glazing type [14,15]. The most common practice is to conduct a parametric investigation of different WWR values based on local climatic conditions and other architectural factors. Several studies have recommended specific WWR values for different school buildings. Alwetaishi et al. focused on the impact of the WWR and its orientation on the indoor environment of schools in Saudi Arabia. They recommended a WWR value of 10% to 20% and choosing the north-facing classrooms for better performance [16], while a WWR range of 30–45% was recommended for selected European cities that represent different European climates [17]. The Saudi Building Code recommends that external glazing does not exceed 50% of the external wall area for educational buildings [18]. However, it is unclear how this could impact building performance regarding daylighting. Moreover, the literature lacks information about the impact of internal daylighting elements, such as courtyards and atria, which are commonly used in Saudi Arabian school buildings.

Daylighting design strategies in school buildings play a crucial role in creating a comfortable and inviting atmosphere. Many dynamic technologies have been offered as alternatives to traditional and static systems to provide appropriate visual comfort [3]. These technologies enable the transparent elements of the building envelope to adapt and respond to the varying illuminance levels between the interior and exterior environment, such as dynamic shading devices [19,20] and advanced smart-glazing window systems [21,22], as well as building typologies, such as the atrium, courtyard [23–25], orientation, and provision of adequate openings. However, in hot climates, excessive glazing in buildings can lead to significant heat gain and visual discomfort; therefore, the existing commercial smart glazing system products, such as polymer dispersed liquid crystal (PDLC) [26], electrochromic (EC) [27] and SPD [28] glazing, can help achieve visual comfort in particular at existing school buildings.

1.1. Smart Glazing System

Smart windows dynamically adapt their characteristics based on external environmental factors or electrical stimuli to regulate indoor conditions. These adaptive changes can be triggered by temperature variations through thermochromic and thermotropic mechanisms, by light via photochromic processes, or by gas changes through gasochromic systems. Alternatively, electrically activated systems such as SPD become transparent when Applied AC electric power is applied to an SPD glazing, which can vary the transmission from 0.1% to 60% at switching speeds of 100–200 ms. Figure 1 provides a detailed explanation of SPD functionality. The key advantage of these adaptive windows lies in their ability to modulate light transmission autonomously, eliminating the need for separate shading solutions and enhancing user comfort.

Research on smart windows, particularly those utilizing SPD, has been explored numerically and experimentally. Aritra et al. have examined SPD test cells' daylighting and thermal attributes under real-world conditions in temperate climates [29–31]. Studies have also been conducted on the energy performance of systems that combine SPD glazing with photovoltaic (PV) technology [32]. However, more research is needed for hot climate contexts like ours. Mesloub et al. carried out a comprehensive analysis of the energy and daylighting performance of SPD glazing in various states compared to conventional double glazing in office buildings. Their findings suggest that SPD smart windows can significantly reduce net energy consumption by up to 58% compared to low-emissivity double glazing. Further data on daylighting and glare effects are essential for future architectural applications of SPD glazing across different building types [28].
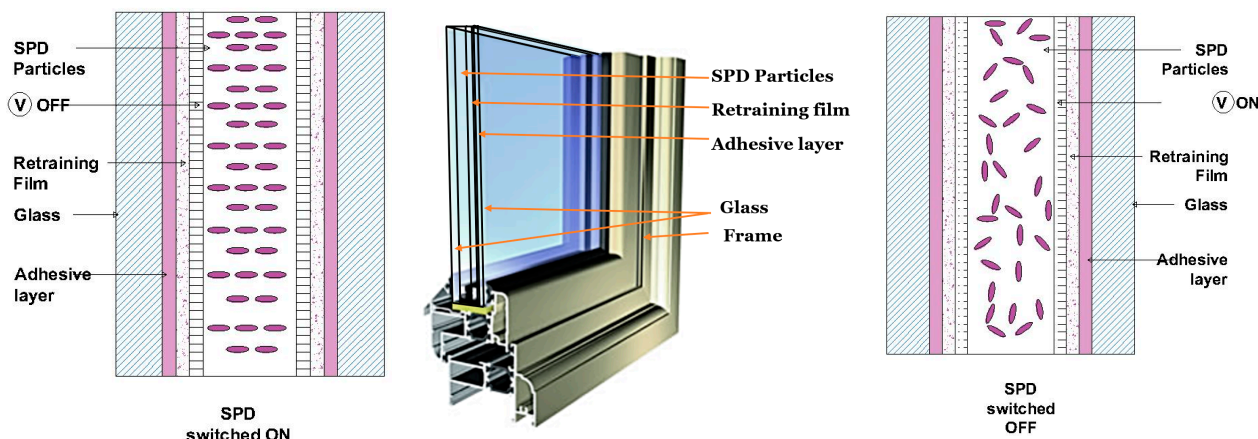
Figure 1. Functionality of SPD glazing in transparent and opaque state. Middle part modified from the reference [33].

1.2. Atrium and Courtyard Typologies

Architectural elements such as atriums and courtyards are pivotal in optimizing daylighting in educational facilities, thereby significantly influencing energy efficiency and the learning environment [34]. Typically situated centrally within a building's layout, an atrium functions as a voluminous, naturally illuminated open space that enhances the lighting conditions of adjacent classrooms. Courtyards, defined by their enclosed yet open character, similarly facilitate daylighting for surrounding educational spaces. These elements not only serve to modulate natural illumination but also act as visual connectors across different architectural layers, engendering a perception of spatial openness and environmental connectivity. The effectiveness of these features can be augmented through strategic design interventions such as the integration of specialized glazing or skylights [35], which aim to maximize natural light influx while mitigating glare and thermal gain issues. Complementary strategies like the incorporation of reflective interior surfaces [36] and automated lighting controls [37] further fine-tune the daylighting performance by respectively enhancing light distribution and dynamically adapting to changing illumination conditions. Therefore, the tactical implementation of these architectural and design components constitutes an essential multi-modal strategy for the enhancement of daylighting performance in educational settings.

In recent years, the impact of atrium and courtyard typologies on optimizing daylighting performance has garnered significant academic attention. Ma and Yang, in 2022, found that for Nanjing's climate, classrooms oriented toward the north and east sides of atriums provided the best daylighting. The study further elaborated that a corridor width of 3 m ensured optimal daylight for the lower floors and even provided design equations for the optimal atrium width and length [34]. Another study conducted by Xue and Liu in 2022 explored the optimal design parameters for commercial atrium daylight quality. This experimental study recognized seven atrium design parameters, including Skylight VT and Wall reflectivity, as significantly influencing daylight quality. These parameters' effects on daylight quality were determined through correlation analysis and multiple linear regression analysis [38]. Further examination into the daylighting parameters for courtyard and atrium buildings revealed combinations beneficial for occupants' well-being. The researchers Talip et al. in 2021 found that a Window-to-Wall Ratio (WWR) of 30%, combined with shading devices, was the most favorable option for daylight performance in the tropical courtyard and atrium buildings [39]. This was supported by Radiance Daylighting Simulations, which solidified the daylight performance outcomes through calculated data modeling. Another intriguing study by Wu et al. in 2021 emphasized the role of the area ratio (AR) and section aspect ratio (SAR) of skylights to roofs. Through simulations, it was determined that these ratios profoundly impact the lighting and thermal environments of

atriums, suggesting that maintaining SAR within a 0.2–0.6 range can enhance the thermal environment without hindering natural lighting [40].

A study conducted by Ferreira et al. in 2019 found that by shifting the atrium from an enclosed structure to a semi-enclosed one, daylight in the adjacent rooms could be doubled without altering the floor area of the building while also indicating that wall reflectance values significantly influence daylight conditions in these rooms [41]. This observation was reiterated in another study in 2018, which proposed that altering the geometrical volume and transitioning the atrium's characteristic from an enclosed to a semi-enclosed structure can effectively increase the daylight quantity in the adjacent spaces [42]. In a related investigation by Yunus et al. (2019), the impact of internal roof obstructions was analyzed, revealing that such obstructions consistently attenuated daylight, especially when compared to clear, unobstructed roofs. Furthermore, complex configurations in unobstructed atrium wells were observed to increase light distribution discrepancies [43]. Emphasizing the importance of design. Another research conducted by Fang and Cho in 2019 introduced an optimization process that underlined the pivotal role of skylight dimensions in enhancing daylighting, concluding that the width and length of skylights were the most influential variables across different locations [44].

Investigating more deeply into the intrinsic attributes affecting daylighting, Potočnik and Košir, in 2021, identified windows as pivotal building elements. More specifically, the WWR and glazing transmissivity were highlighted as the most influential geometrical and optical parameters, especially for occupant positions located deeper inside a space and oriented away from windows [45]. The impact of daylight in atrium spaces on individuals' emotional and psychological well-being is also noteworthy. This was emphasized in a study that analyzed the international design experience of daylight in atrium spaces characterized by climates similar to Russia [46]. The research accentuated how the physical factors of atrium space daylight profoundly affect the architectural space-planning design and the emotional perception of those within the space.

Various methods and analytical approaches have been employed to optimize building performance in terms of daylighting. A study proposed a predictive method for determining daylight factors, boasting an impressive average accuracy of over 90% [47]. This method utilized measurements from scale models and real courtyards under authentic overcast conditions to define these factors, subsequently leading to quantifiable energy savings in electric lighting. In separate research focused on China, it was revealed that fully air-conditioned atria were highly energy-consuming, especially due to their air-conditioning needs. However, researchers determined through field measurements and computational simulations that an atrium's geometric configuration heavily influenced its indoor thermal condition and overall energy consumption [48]. Advances in simulation have also enabled more comprehensive insights. For instance, a study leveraging simulation techniques deduced that the WWR was not a major determinant of indoor daylight hours. Instead, internal courtyards were found to significantly enhance illuminance hours, particularly during shorter days when light is paramount [49]. Such findings underscore the importance of integrating innovative methods and deep analysis to optimize daylighting performance in atrium and courtyard typologies.

Despite the extensive body of literature elucidating the significance of daylighting parameters, geometrical and optical attributes, and their impacts on atrium and courtyard typologies, there needs to be more research regarding the application of smart windows in educational buildings, particularly about visual comfort within these spaces. Here is a justification for addressing this gap in the context of Saudi Arabia:

- Climatic Specificity: Saudi Arabia's climate is marked by extreme solar radiance and long sunshine during the day. This climatic specificity demands unique architectural solutions to achieve visual comfort. The implementation of smart windows in atriums and courtyards of educational buildings can dynamically respond to the varying daylight conditions of the country, ensuring optimal comfort and energy efficiency.

- Cultural Significance of Atriums and Courtyards: Atriums and courtyards are not mere architectural features in Saudi Arabia but have deep-rooted cultural significance, often serving as community gathering spaces. Enhancing visual comfort in these areas not only elevates the functional quality but also augments the cultural value of these spaces.
- Educational Building Emphasis: The importance of daylight in educational spaces cannot be overstated. The right amount and quality of daylight can boost the cognitive abilities and well-being of students. Given the rapid expansion and investment in the educational sector in Saudi Arabia, there's an imperative to ensure that these spaces are designed for maximum student benefit.

This research aimed to develop an optimized school model concerning the current visual comfort issues of classrooms in Saudi Arabia, which would align with the Saudi Vision 2030 programs strategy to ensure healthy future development standards and improved performance of its indoor environmental quality. Also, this study may benefit in advancing designers' knowledge and impact decision-making when developing new school projects with an indoor visual environment. Thus, this study has focused on the optimization of multiple physical architectural elements of classroom school design, such as WWR of skylight, WWR of external glazing, floor levels, and switching mode of SPD, to have a holistic perspective of the conditions of the current and new-pilot school models. The visual comfort parameters in the scope of the study are determined by the daylighting quantity and quality, such as point in time illuminance (WPI), uniformity index (Ui), Climate-based annual metrics (Useful Daylight Illuminance (UDI) thresholds and Spatial Daylight Autonomy (sDA), and Daylight Glare Probability (DGP)).

Hourly evaluations can identify specific time intervals that might present visual discomfort due to factors such as direct sunlight penetration, glare, or insufficient natural light. Metrics such as dynamic daylight simulations often aid in hourly evaluations by tracking daylight availability and quality throughout the day [50]. On the other hand, annual metrics, like Daylight Autonomy (DA) and Continuous Daylight Autonomy (cDA), offer a holistic view by estimating the percentage of annual occupied hours when classrooms receive sufficient daylight [51]. Moreover, the Useful Daylight Illuminance (UDI) aids in understanding both under-lit and over-lit conditions annually, emphasizing the balance between adequate and excessive daylight [35,52]. Implementing these metrics in classroom design facilitates an environment conducive to learning, minimizing disruptions due to visual discomfort. The optimization of daylighting in architectural design involves achieving a balance between providing sufficient natural light and avoiding undesirable effects such as glare or overheating. UDI is often regarded as a more comprehensive metric for daylighting optimization compared to others due to providing detailed assessment across a spectrum, where this spectrum-based approach provides a fuller picture of how spaces experience daylight throughout the day and year and also supports holistic design decisions; with UDI's comprehensive assessment, designers can make holistic decisions about window orientation, glazing types, shading devices, and other design elements to create spaces that harness daylight effectively and comfortably. In summary, when it comes to daylighting optimization, UDI provides a more detailed assessment of daylight conditions than many other metrics. Therefore, a more effective approach to optimizing daylight in architectural spaces. In this study, DGP was chosen over Unified Glare Rating (UGR) as the glare indicator because DGP is specifically designed for evaluating glare in spaces primarily lit by daylight. DGP considers both direct and indirect sunlight, making it more suitable for assessing visual comfort in environments with significant natural light, which aligns with this study's focus on daylighting and advanced glazing systems. Unified glare rating (UGR) is typically used for assessing glare from artificial lighting sources. While it is a valuable metric, it does not account for the complexities of natural light, such as varying intensities and angles of daylight throughout the day.

2. Methodology

Computational techniques can successfully gather qualitative and quantitative components of architectural performance and optimize a form once constructed to integrate the parametric design approach to the building's visual context.

This study describes the parametric design process of integrated SPD smart glazing in several school typologies to be produced in Rhino-Grasshopper, honeybee-for-radiance, and Colibri 2.0 from CORE Studio included in TT Toolbox then exported to design explorer for evaluation and daylighting optimization. The combination of these tools was required to achieve the study's aims. The daylight analysis method employs Rhino7 as a modeling tool, Grasshopper, as a parametric interface, Honeybee, and Honeybee-radiance (create, visualize, Bidirectional Scattering Distribution Function (BSDF) modifier for SPD states to accurately represent the complex light scattering and transmission properties and other input reflection and transmission materials, iterate). The design explorer allows the selection of potential optimal classroom models for further investigation in several school types, including courtyard, atrium with skylight and atrium with clerestory.

This study uses a bilateral lighting mode with south and east-facing classrooms within a specific schedule period and in the city of Hail, Saudi Arabia, as a case study to examine the actual daylighting performance for reference models as detailed in Table 1, and then compare with optimized models' potential for establishing an indoor visual comfort environment. This is done with the intention of organizing the research flow of this study in three stages, as presented in Figure 2.

Table 1. Description of the main components of typologies.

Typology Components	Characteristic
Classroom dimension	9 m × 6 m × 3 m
WWR external window	20%
WWR internal window	50%
Glazing type	Double glazing air
Skylight material	Acrylic

Stage 1: Extract the optical transmission data of different spectrum SPD switchable glass systems for usage as an alternate glazing system for exterior and glass for daylighting stage optimization.

Stage 2: Parallel to the parameterization of the three school prototypes, a list of critical visual comfort preferences that lead to daylighting performance is developed by integrating SPD switchable glazing instead of reference glass with varying transparency and WWR of external glazing facade and skylight in the case of the atrium. Based on the input variables, the algorithm generates all potential design options using an evolutionary solver named colibri2.0 to further evaluate the annual daylight meter ($UDI_{300lux-1000lux}$) based on the educational buildings schedule in Saudi Arabia.

Stage 3: The daylight glare probability (DGP) analysis is performed for the best-performing design options from the preceding steps, using the different transmissions of SPD switchable glazing. The hemispherical fisheye camera (180°) was chosen and put near to east and south-facing windows in classrooms. However, all rendered images are displayed in false color on a logarithmic scale.
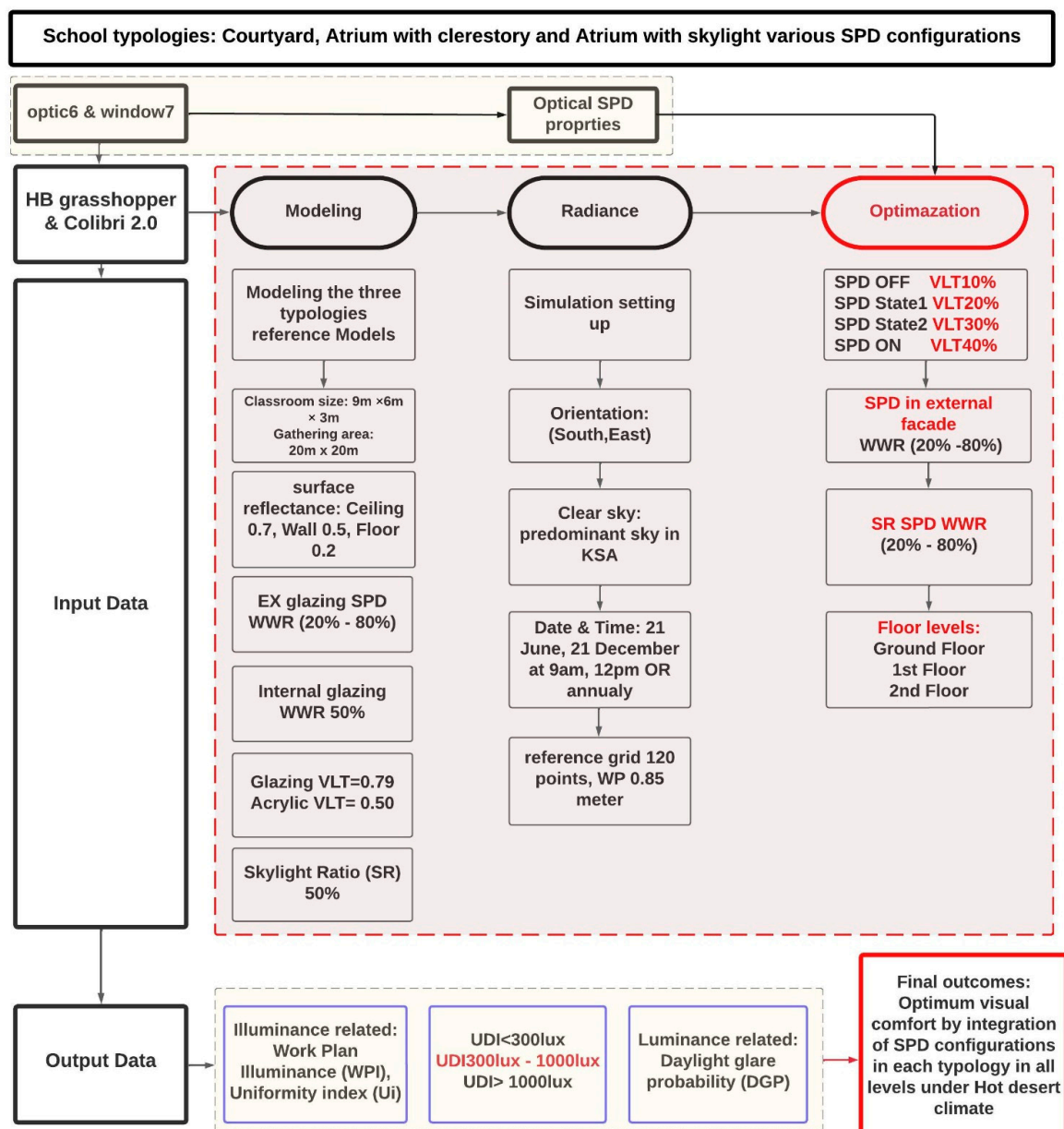
Figure 2. Methodology flowchart.

2.1. Modeling Reference Cases

1. *The atrium with skylight configuration:* This typology comprises a square atrium (20 m × 20 m) in the center, and the design includes three stories and corridors with a 2 m depth on each floor. Each classroom inside the walls has an internal window. Consequently, Daylight enters the classroom via the windows positioned on the exterior elevations and the internal window that is connected to the top peripheral atrium openings, as presented in Figure 3.

2. *The courtyard configuration:* Anchoring this typology is a central square courtyard measuring 20 m × 20 m. Light bilaterally permeates the space. Interestingly, an internal 2 m corridor acts not just as a passageway but also as a shading element, functioning akin to an overhang.

3. *The atrium with clerestory configuration:* this typology is characterized by an enclosed atrium punctuated with peripheral openings placed strategically on the higher sections of the walls. Daylight ingress is curated through the classroom's external fenestration and the elevated clerestory sections.
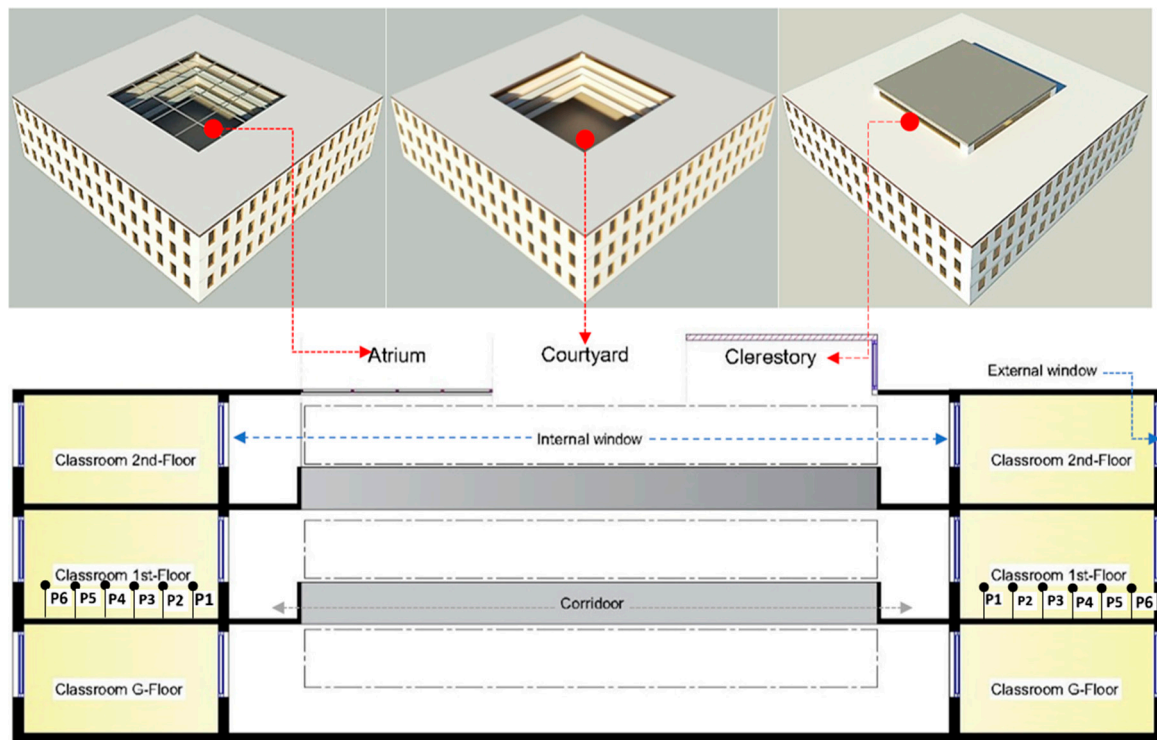
Figure 3. Three-dimensional and section of different daylighting typologies and disposition of workplane illuminance points.

2.2. Description of SPD Glazing

In the present study, an SPD glazing system from Smart Glass International was utilized, necessitating an electrical input of 110 V AC to attain full transparency. Notably, zero power input was required to transition to an opaque state, with a nominal energy consumption of 5 W/m^2 for the actuation between states. The optical properties of the SPD glazing—both in its transparent ('ON') and opaque ('OFF') states—were comprehensively characterized using an AvaSpec-ULS2048 spectrometer, as depicted in Figure 4. The optical metrics were quantified through the application of Equations (1) and (2), which delineate the luminous and solar transmittance, respectively.

$$\textit{Luminous transmission} \qquad \tau_V = \frac{\sum_{\lambda=300nm}^{780nm} D_{65}(\lambda)T(\lambda,\alpha)V(\lambda)\Delta\lambda}{\sum_{\lambda=300nm}^{780nm} D_{65}(\lambda)V(\lambda)\Delta\lambda} \tag{1}$$

$$\textit{Solar transmission} \qquad \tau_s = \frac{\sum_{\lambda=300nm}^{2500nm} S(\lambda)T(\lambda,\alpha)\Delta\lambda}{\sum_{\lambda=300nm}^{2500nm} S(\lambda)\Delta\lambda} \tag{2}$$

D_{65}, $V(\lambda)$, $S(\lambda)$, and $\Delta\lambda$ and $T(\lambda)$ signify the relative spectral distribution of the D65 illuminant, the spectral luminous efficiency of a standard photopic observer, the spectral distribution of solar irradiance, the wavelength interval, and the spectral transmission properties of the glazing material, respectively.

Experimental data revealed that the solar reflection indices for the SPD system in the 'ON' and 'OFF' states were consistent at 9%. Furthermore, transmittance values in the visible spectrum were documented at 43% and 11% for the 'OFF' and 'ON' states, correspondingly. Concurrently, reflectance indices registered at 8.2% and 6.8% for the respective states. Building upon the prior optical characterization, a dimmer switch was integrated into the SPD glazing system to enable variable transmittance settings. In this investigation, the transmittance values were strategically chosen to range from 10% to 40%, representing extreme operational cases. The rationale for selecting a 10% interval was multifold:

1. It provides a sufficiently granular yet manageable spectrum of states to evaluate the energy and optical performance of the SPD glazing.
2. This range covers the critical thresholds for luminous and solar transmittance in practical applications, ensuring that the results are not only academically rigorous but also industrially relevant.
3. Employing a 10% interval creates a balanced trade-off between computational workload and analytical precision, thus facilitating a robust understanding of the system's behavior across different operational states.

Therefore, the chosen interval serves as an effective framework for systematically studying the dimmable capabilities and performance implications of the SPD glazing system.
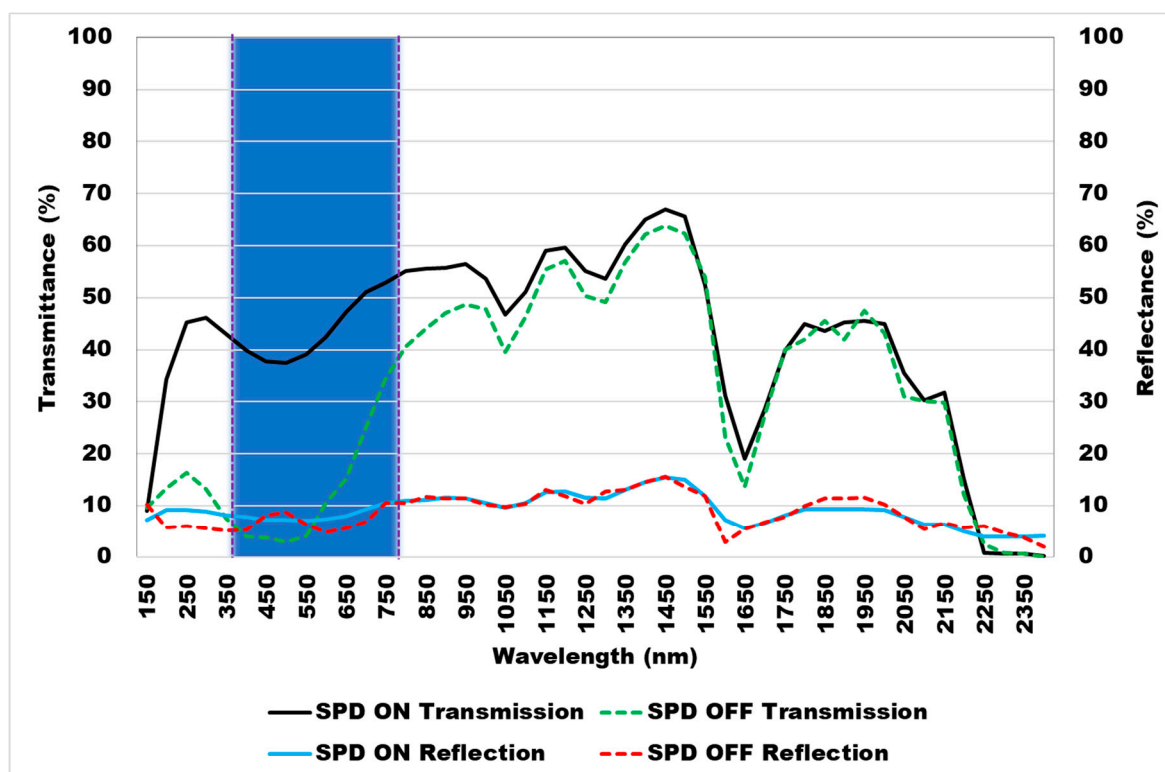
Figure 4. Normal-hemispherical spectral transmittance and reflectance of SPD window in its ON (transparent) and OFF (opaque) states.

2.3. Radiance Computer Simulation

The simulated WPI values were tabulated between the south–north bilateral window in the middle grid. In addition, the Ui of interior daylight, which is the ratio of average illumination to maximum illumination, was utilized to determine the quality of daylight distribution. According to the NBN L13-001 code and international regulations [34], this ratio shall not exceed 0.6 above the work plane. Simulations were conducted to analyze the annual variation and the critical period within the design days during the summer and winter solstices (21 June, 21 December) and between 9:00 a.m. and 12:00 p.m.

Also, the annual daylight availability for three successive levels of a typical classroom was recorded for each kind. We conducted a sensitivity analysis for different daylight modeling options and Radiance definitions to determine the optimal balance between accuracy and calculation time; this analysis informed our decision to perform daylight calculations for an open floor plate with a 1m dense sensor grid and six ambient bounces. While this study focuses on the integration of SPD switchable glazing (self-shading) in comparison to the daylight availability of reference models, the daylight analysis was

performed without shading devices.However, the total of iterations for simulation 6144 as depicted in details in Table 2.

Table 2. The input variables used in daylighting optimization.

Input Parameter	Units	Values	No. of Iterations
Model typologies	-	Courtyard, Atrium with skylight, Atrium with clerestory	3
Orientation	-	South, East	2
Floor number	-	3 levels	3
WWR external window	%	20, 40,60, 80	4
WWR skylight	%	20, 40,60, 80	4
VLT of SPD	%	10, 20, 30, 40	4
Total of iterations			6144

The selection of simulated points (grids) within classrooms corresponded to the grids plotted according to the layout of work planes. The minimum number of points required in each classroom was 120 sensors at a height of 0.85 m. As illustrated in Figure 2, the space between the simulated grid points was maintained at 1m to ensure accurate findings. The hemispherical fisheye camera (180°) was chosen and placed near classroom windows facing east and south. On a logarithmic scale, however, all produced images take on a false color.

3. Results and Discussion

3.1. Daylighting Level Distribution

3.1.1. Courtyard Typology

Analyzing the illuminance distribution of different classrooms (P1–P6) in various façades (east, south, west, north) and floors (ground, first, second) of courtyard typology in schools across two different periods (9.00 a.m. and 12.00 p.m.) and in two distinctive seasons (solstice summer and solstice winter), reveals a myriad of trends and patterns.

The eastern façade's overall illuminance values are generally higher during the morning hours compared to noon for both summer and winter. In solstice summer at 9.00 a.m., the highest illuminance is observed in the P6 classroom (9157 lux on the ground floor), indicating significant sunlight exposure at this hour. The illuminance gradually reduces as we move upward through the floors, suggesting a probable shadowing effect due to the architecture of the building. Contrarily, in solstice winter at 9.00 a.m., the P2 classroom shows the highest illuminance on the ground floor (3245 lux), surprisingly higher than the summer values, suggesting perhaps a lower sun angle and less shadowing during winter mornings. Noon values for both summer and winter show a significant drop in illuminance, with P6 again recording the highest summer value (1345 lux on the ground floor) and P2 the highest winter value (648 lux on the second floor). The southern façade presents a starkly different scenario, with the highest illuminance values observed at noon during winter, predominantly in the P1 classroom. The high winter illuminance could be attributed to the lower sun path in winter months allowing more direct sunlight on southern exposures. During summer, the illuminance peaks in the morning at P1 (ground floor: 874 lux) but is much lower than the winter values. The noon values in summer are generally higher than the morning values, with the P1 again having the highest illuminance. The western façade follows a similar pattern to the eastern façade, with the highest illuminance occurring in the morning hours. However, The winter illuminance values are notably higher, particularly in the P4 classroom. This indicates a strong exposure to the afternoon winter sun which would be lower in the sky and thus more directly incident on the façade. At noon, the values drop significantly for both seasons but follow a similar pattern, with the highest illuminance at P2 in summer and P2 in winter. Finally, the northern façade presents an interesting pattern with relatively low illuminance values in summer but extremely high

values in winter, especially at noon. This could be attributed to the northern façade's exposure to indirect, diffused light during summer and direct sunlight during winter due to the lower sun path. The highest winter illuminance is observed in P1 at noon (ground floor: 27,024 lux), which is considerably higher than other readings, indicating a strong winter sunlight exposure. Conversely, the highest summer illuminance is noticed in P6 at noon (ground floor: 1687 lux) as presented in Figure 5.

The Ui data for the courtyard typology exhibits distinct performance patterns across different orientations and floors, as depicted in Figure 6. For the eastern facade, all floors surpass the 0.6 Ui standard throughout the day during both summer and winter solstices, showcasing a strong performance of illuminance delivery. The southern façade's Ui values fall below standard during winter but remarkably outperform in summer, particularly during morning hours. The western façade demonstrates impressive uniformity in both solstices, consistently exceeding the standard Ui, while the northern façade exhibits exceptional performance in summer but struggles to meet the standard during the winter solstice. Therefore, it is evident that while courtyard typology generally provides strong uniformity of illumination, specific orientations and seasons can impact performance significantly.
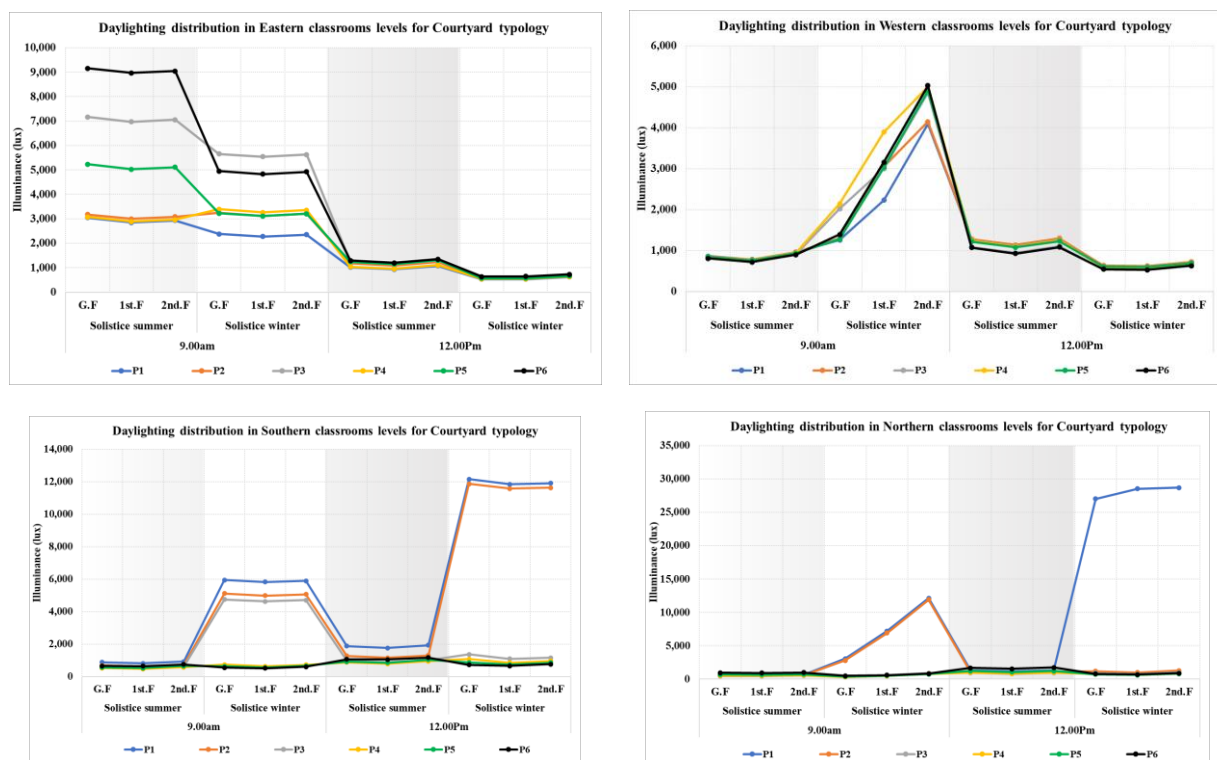
Figure 5. Daylighting distribution point in time illuminance for reference classrooms in cardinal orientation for courtyard typology.

3.1.2. Atrium with Skylight Typology

Figure 7 illustrates the patterns of illuminance distribution across diverse floors of an atrium typology at two critical time points, 9.00 a.m. and 12.00 p.m., during the summer and winter solstices and across the cardinal orientations. The eastern façade's illuminance exhibits an expected diurnal and seasonal pattern. It peaks at 9.00 a.m. during the summer solstice, with values exceeding 8900 lux at Point 6 (P6) on all floors, attributable to the incident morning sunlight. Contrastingly, the winter solstice presents significantly subdued illuminance, with the zenith at 481 lux, an outcome of the sun's lower altitude. As the day progresses to 12.00 p.m., the summer illuminance recedes, paralleling the sun's shift toward the western façade. Notably, the illuminance values, ranging between 300 to 1000 lux across all points, are maintained owing to the consistent internal window-enabled

daylight penetration from the atrium. On the southern façade, at 9.00 a.m., the summer illuminance is relatively diminished compared to the eastern façade. However, in winter, an exceptionally heightened illuminance surpassing 11,900 lux is recorded at P1 on both ground and second floors, likely driven by the atrium skylight's direct sunlight penetration. At 12.00 p.m., the summer illuminance experiences a surge, culminating at 1720 lux at P1 on the ground floor, in alignment with the sun's zenith. Conversely, winter readings retain their elevated levels, witnessing a marginal increase from their 9.00 a.m. counterparts. The western façade demonstrates significantly lower illuminance levels at 9.00 a.m. during the summer solstice, relative to the eastern and southern façades. The apex reading of 465 lux at P1 on the ground floor is attributed to the reflective contribution of incident sunlight from the ground. This is a predictable outcome considering the sun's eastern sky position at this hour. Correspondingly, winter illuminance levels are also lowered, with a maximum of 451 lux observed at P2 on the Ground floor. By 12.00 p.m., the western façade experiences an increase in illuminance with the sun's westward shift, reaching a summer peak of 865 lux at P1 on the first floor. Winter illuminance levels, in contrast, register a minor decrease from their 9.00 a.m. levels. The northern façade's illuminance at 9.00 a.m. during the summer solstice is considerably lower than its cardinal counterparts, an effect of the sun's path. The zenith value of 864 lux is observed at P6 on the ground and first floors. Intriguingly, the winter illuminance at P1 on the ground floor and second floor drastically exceeds 8000 lux, potentially facilitated by the bilateral lighting typology's internal window-directed sunlight penetration. At 12.00 p.m., summer illuminance values demonstrate a significant amplification, especially at P6, ascending to 1524 lux on the Ground floor. In contrast, winter values at P1 register a subtle decrement from their 9.00 a.m. levels yet remain extraordinarily elevated relative to the remaining points. Overall, the distribution of illuminance across the atrium typology under study presents complex yet decipherable diurnal and seasonal patterns. These patterns manifest a crucial interplay of the atrium's architectural features, including the internal windows and the skylight, along with the sun's cardinal position, yielding critical insights into efficient daylight utilization.
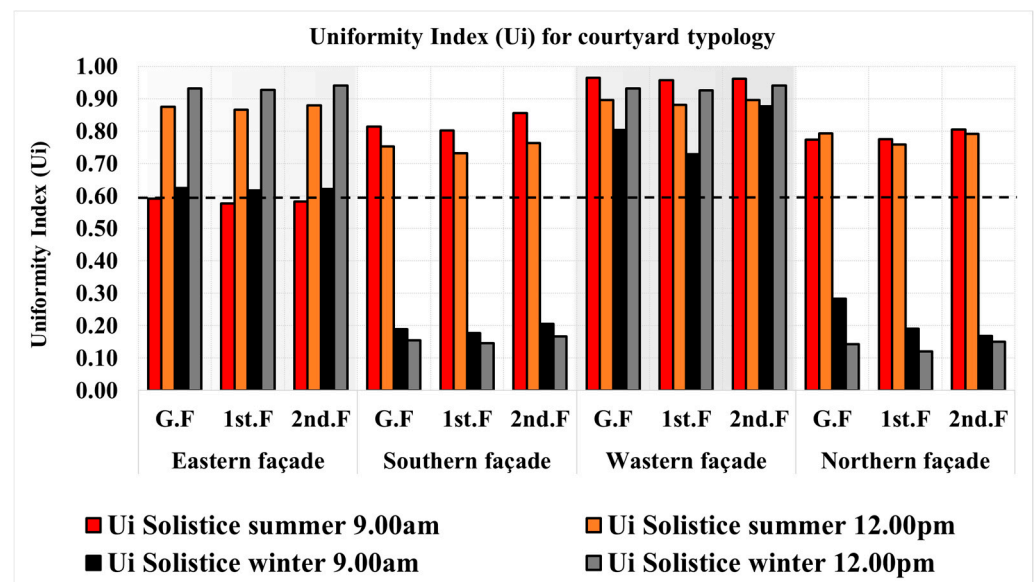
Figure 6. Ui for courtyard typology in cardinal orientation.

Assessing the Ui of an atrium typology in classrooms during solstices, an examination of cardinal orientations and distinct times reveals a variation in daylight distribution, as presented in Figure 8. The eastern façade meets the recommended Ui standard (>0.6) only during noon in the summer and at both observed times in winter. Conversely, the southern façade underperforms, only exceeding the standard in one instance, at 9.00 a.m. on the first floor during summer, while dramatically falling short in winter due to high daylight

contrasts. The western façade demonstrates consistently high uniformity in all scenarios, underscoring its capacity to facilitate balanced daylight penetration. Lastly, the northern façade generally fails to meet the standard in summer but exhibits an improvement at noon on the first floor, whereas winter values remain below standard except for the second floor at noon. These outcomes highlight the significance of orientation and seasonality in maintaining optimal uniformity of illuminance in atrium-designed classrooms.
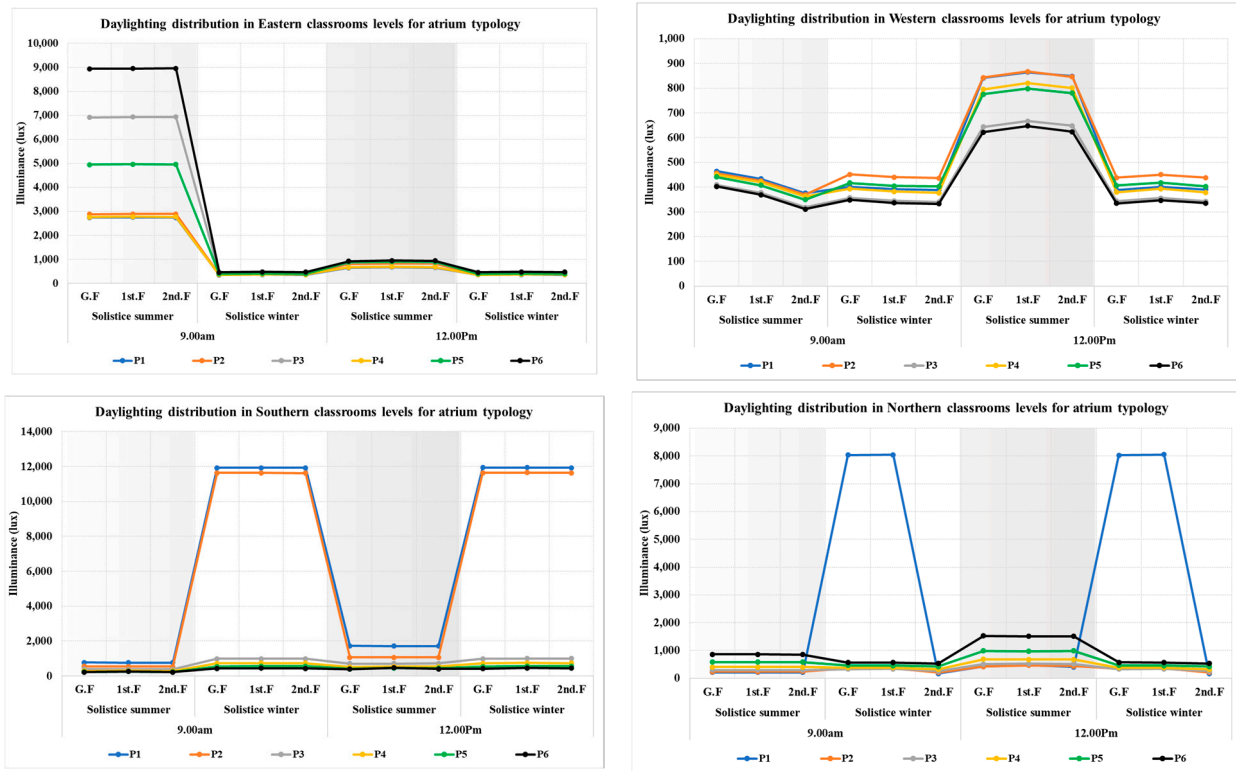

Figure 7. Daylighting distribution point in time illuminance for reference classrooms in cardinal orientation for atrium with skylight typology.
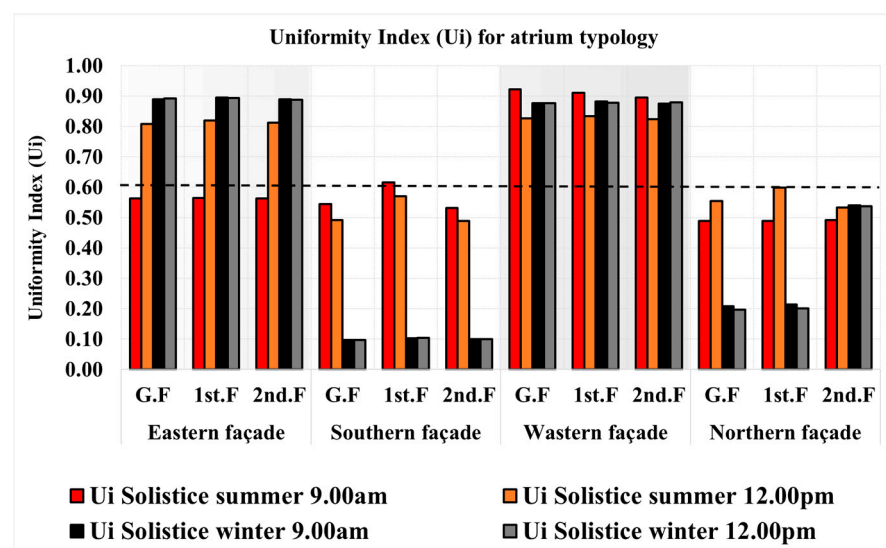
Figure 8. Ui for atrium with skylight typology in cardinal orientation.

3.1.3. Atrium with Clerestory Typology

Upon analysis of the illuminance distribution for classrooms in the atrium with clerestory typology school building, several interesting patterns and comparisons emerge. The data presents illuminance levels at 9.00 a.m. and 12.00 p.m. across both solstice summer and winter, factoring in cardinal orientations (east, south, west, north) and the floors of the building (ground, first, and second).

On the eastern façade, P6 consistently reports the highest illuminance during summer solstice across both times of the day. The 9.00 a.m. Figure 9 are remarkably high, suggesting that these classrooms may experience strong morning sunlight during this season. Interestingly, during the winter solstice, P4 shows the highest illuminance at 9.00 a.m., but P2 outperforms the other classrooms at noon. This could be due to differences in the sun's position and intensity during these periods. On the southern façade, the P1 classroom exhibits the highest illuminance at both times and seasons. Notably, at noon during winter solstice, the values are remarkably high, peaking at 11,960 lux on the second floor. This trend suggests that these classrooms experience significant light exposure, particularly during midday in the winter. In contrast, on the western façade, the 9.00 a.m. Figures are relatively modest across all classrooms and seasons. However, there's a significant increase in illuminance at noon during the summer solstice, with the P1 and P2 classrooms having the highest values. During the winter solstice, P1 and P2 also exhibit the highest illuminance, but at 9.00 a.m. These observations suggest that classrooms on the western façade may benefit from ample afternoon sunlight during summer and morning sunlight during winter. The northern façade illuminance is overall lower in summer at both time intervals compared to other façades, which is expected due to the sun's trajectory. However, during winter, the illuminance increases significantly, with the P1 classroom showing the highest illuminance at 9.00 a.m. and the P6 at noon. The highest value reaches up to 1577 lux in P6 at noon, suggesting substantial sunlight exposure during this period. Upon comparing the different façades, it appears that the southern façade experiences the highest illuminance during winter, particularly at noon, while the eastern façade has the highest illuminance during summer mornings. The western façade tends to receive the lightest in the afternoon during summer and in the morning during winter. The northern façade has overall lower illuminance levels in summer but experiences a substantial increase during winter, especially at noon. The variation in illuminance between the ground, first, and second floors is relatively small for all façades. However, there's a general trend of slightly increasing illuminance with the rise in floor levels. This could be due to lesser obstruction to sunlight at higher levels.

Figure 10 illustrates the Ui in various orientations and floors of the clerestory typology. For the eastern facade, every floor at every timepoint during winter achieves the standard Ui of 0.6 or higher, while during summer, this threshold is only met on the second floor at noon. In contrast, the southern façade presents winter results below the standard, although the second floor demonstrates improved Ui levels during summer, particularly at noon. The western façade exhibits excellent Ui values exceeding 0.82 across all floors during summer, and apart from the ground floor at 9.00 a.m., achieves satisfactory results in winter, too. The northern façade, however, struggles to meet the 0.6 Ui standard during summer, while the second floor somewhat compensates with better Ui results during winter.

3.2. Annual Daylighting Assessment

Figure 11 provides an insightful depiction of the evaluation process of metrics derived from climate-based daylight modeling, with a particular focus on Useful Daylight Illuminance (UDI) and Spatial Daylight Autonomy (sDA$_{300lux}$). This evaluation process is undertaken across classrooms distinguished by their orientations (south, north, east, west) and their location on different floors (Ground, first, second). In the study, three architectural configurations are considered, namely, atrium with skylight and clerestory and courtyard models, all having a WWR of 20%. The subsequent analysis offers a yearly overview of daylight conditions specific to each architectural design.
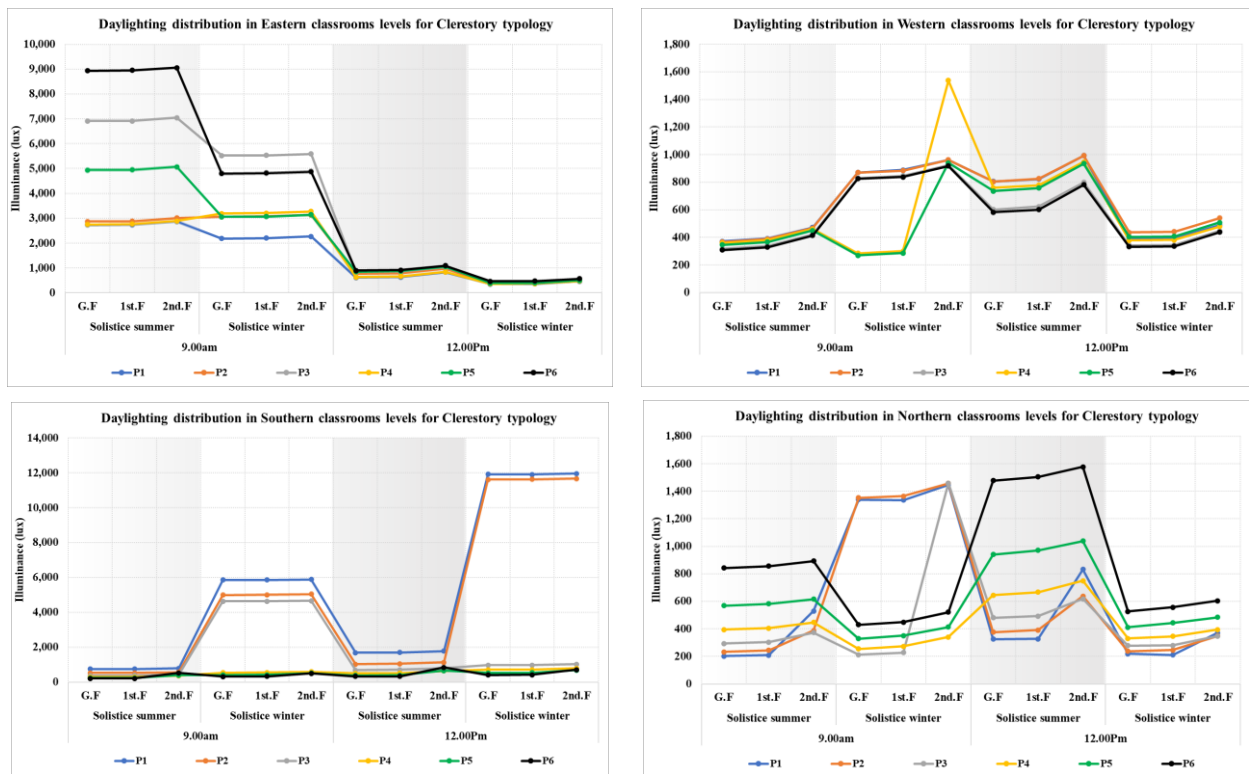
Figure 9. Daylighting distribution point in time illuminance for reference classrooms in cardinal orientation for atrium with clerestory typology.
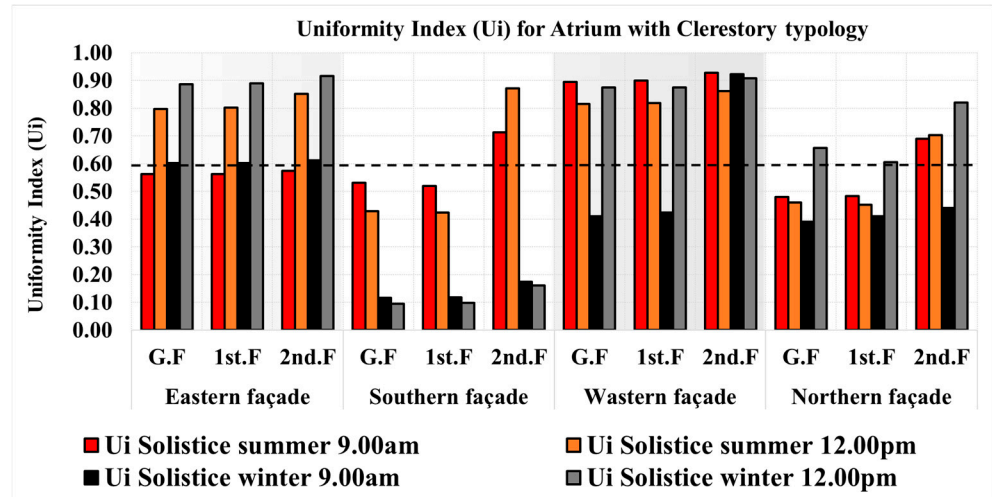

Figure 10. Ui for atrium with clerestory typology in cardinal orientation.

In the case of the atrium-oriented model, the UDI metrics denote that a substantial period of classroom time falls within the $UDI_{300-1000lux}$, deemed as the acceptable range of daylight. Ground-level classrooms with a north-facing orientation witness a higher percentage of time within this acceptable UDI range (66%), while those oriented to the south exhibit a higher instance of excessive brightness (28%). Classrooms located on the first floor adhere to a similar distribution pattern, albeit with a slightly higher presence within the acceptable $UDI_{300-1000lux}$ threshold. In contrast, classrooms on the second floor register an increased occurrence of both extreme brightness and insufficient light, with north-facing classrooms notably displaying the highest percentage of suboptimal light conditions (27%). The atrium itself is excessively bright 46% of the time, indicative of a high likelihood of glare. In terms of sDA_{300lux}, a vast majority of classrooms exhibit a

commendable level of daylight autonomy, with values ranging from 80% to 92%. These values imply that a satisfactory level of daylight is accessible in these classrooms for most of the year. Nevertheless, north-oriented classrooms on the second floor display the lowest sDA_{300lux} value (72%), indicating a requirement for refined daylighting approaches.
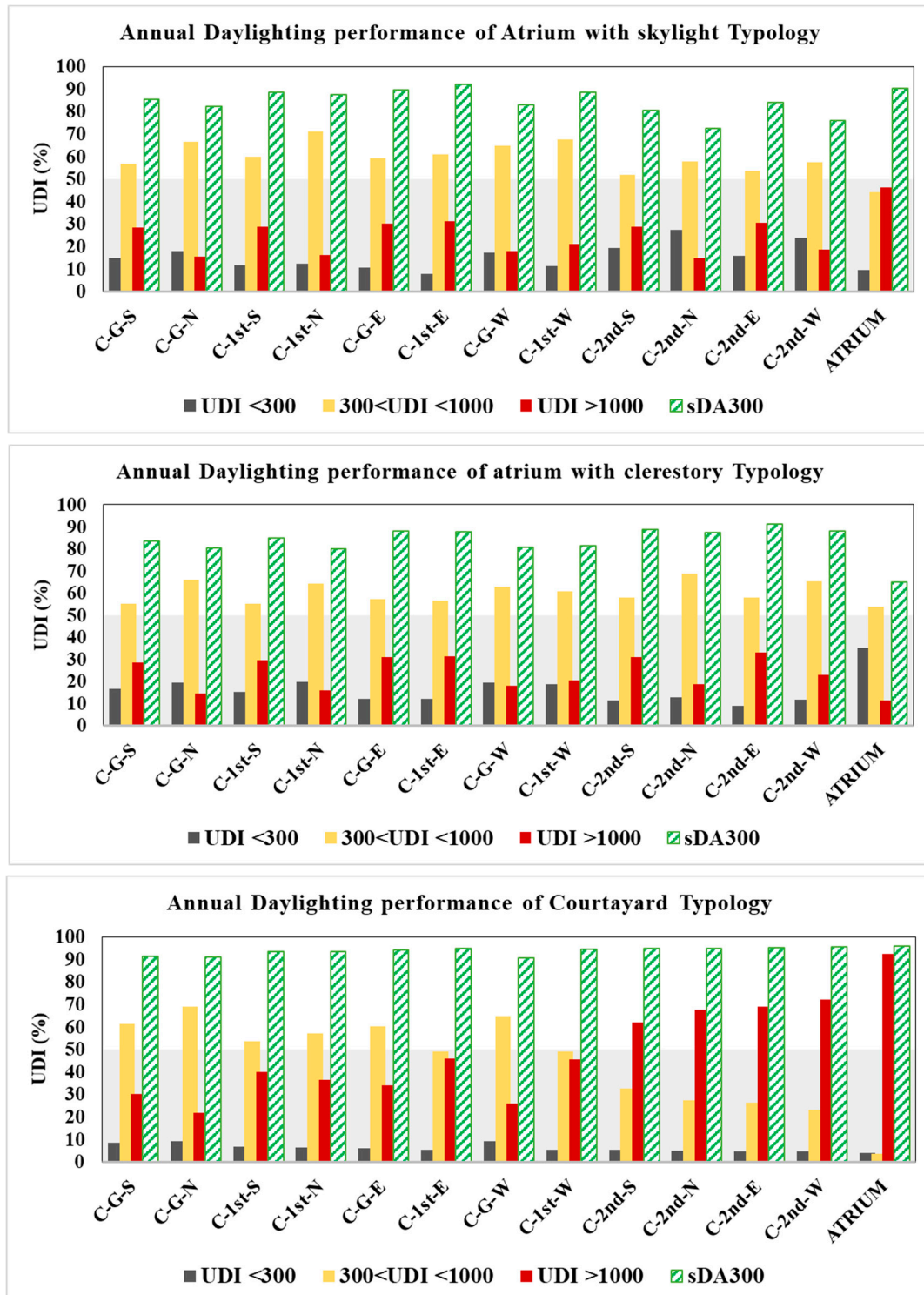
Figure 11. Comparison of UDI thresholds and sDA_{300lux} of different school typology reference models, In the abbreviations, the first letter (C) denotes 'Classroom', the second letter indicates the floor level (e.g., G for Ground), and the last letter represents the orientation (e.g., E for East).

Transitioning to the clerestory model, variations in UDI values are also evident across orientations and floor levels. The $UDI_{<300}$ values fluctuate between 8% and 19%, the $UDI_{300-1000lux}$ values span from 55.09% to 68.80%, and the $UDI_{>1000lux}$ values range from 14% to 33%. The sDA_{300lux} values oscillate between 80% and 91%. According to these results, the $UDI_{300-1000lux}$ distribution predominantly falls within the acceptable range for most classrooms, whereas the atrium area demonstrates a significant percentage of inadequate illuminance, reaching up to 35%. At the same time, the $UDI_{>1000lux}$ records the optimal scenario among the tested typologies. Unmistakably, the sDA_{300lux} values in the clerestory model are inferior compared to the other models, with the atrium exhibiting the lowest value at 65%. This observation further corroborates the balanced daylight distribution in classrooms and the atrium.

Examining the courtyard model, classrooms typically register a significant surge in the excessive $UDI_{>1000lux}$ threshold with the progression of floors. Classrooms on the second floor experience excessively bright conditions more than 60% of the time, specifically in the west-facing classrooms (72%). The atrium is predominantly overly bright (92%). The sDA_{300lux} values are high, comparable to those of the atrium model, signifying commendable daylight autonomy. However, the elevated percentages in the excessively $UDI_{>1000lux}$ threshold hint at potential glare issues, thus emphasizing the need for the deployment of shading strategies.

3.3. Optimization Models

In this section, we examine the repercussions of integrating an SPD switchable glazing system on $UDI_{300lux-1000lux}$ attainment. This system was evaluated in distinct transparency states (from 10% to 40%) and a variety of WWR in educational facilities' east and south-facing classrooms, with an architectural emphasis on courtyard typology. This investigation also included the influence of overhead illumination, such as skylights and clerestory windows, particularly within atrium typology across varying floor levels.

Figures 12 and 13 present an array of design configurations within a courtyard architectural typology, wherein the integration of an SPD switchable glazing meets the minimal $UDI_{300lux-1000lux}$ requirements across all floor levels. However, the lowest transparency state of the SPD system (10% visible light transmission, VLT) fell short of delivering sufficient daylighting across all WWR in both orientations. Interestingly, the juxtaposition of the remaining SPD states with various WWRs yielded between 26 to 32 configurations, from a total of 256, which successfully achieved over 50% $UDI_{300lux-1000lux}$ across all floor levels of the east and south facades. A noteworthy finding revealed that configurations involving the fully transparent state of the SPD system (40% VLT), in conjunction with small WWRs (ranging from 20% to 40%), emerge as efficient daylighting strategies within a courtyard typology. Moreover, the most optimum daylighting conditions were discovered in east and south-facing classrooms, with 40% WWR on the ground floor and 20% WWR on the upper floors, as illustrated in the highlighted sections of Figures 9 and 10. Concurrently, the integration of the SPD system at an intermediate state (20% VLT) also provided an acceptable range of $UDI_{300lux-1000lux}$ when paired with larger WWRs (up to 80%). It is important to highlight the significant role played by the interior corridor that connects classrooms on each floor. Acting as an interior window shading element, it helps achieve a balanced illuminance level, particularly with the bilateral lighting mode in the east-facing classrooms. This critical component of the design serves to maximize daylighting benefits and further supports the flexible and adaptable use of SPD switchable glazing systems in educational facilities. A significant drawback to the courtyard typology, however, lies in the exposure of students' gathering areas to direct sunlight predominantly from 10 a.m. onwards till the school day. This overexposure to sunlight, often associated with heightened temperatures and glare, can adversely impact the comfort and well-being of pupils, potentially impeding their learning environment, in particular in hot climates.

Transitioning to the centralized atrium typology, a comprehensive analysis of 1024 atrium configurations revealed that only 120 and 143 configurations achieved a $UDI_{300lux-1000lux}$ percentage exceeding 50% in eastern and southern classrooms, respectively (refer to Figures 14 and 15). The optimal configuration for both orientations involved an SPD in-

termediate2 transmittance of 30%, combined with a WWR of 40% on the ground and first floors and a WWR of 20% on the upper floor. In addition, a large skylight ratio of 80% interacting with internal windows was employed, resulting in $UDI_{300lux-1000lux}$ values ranging from 62% to 72%.
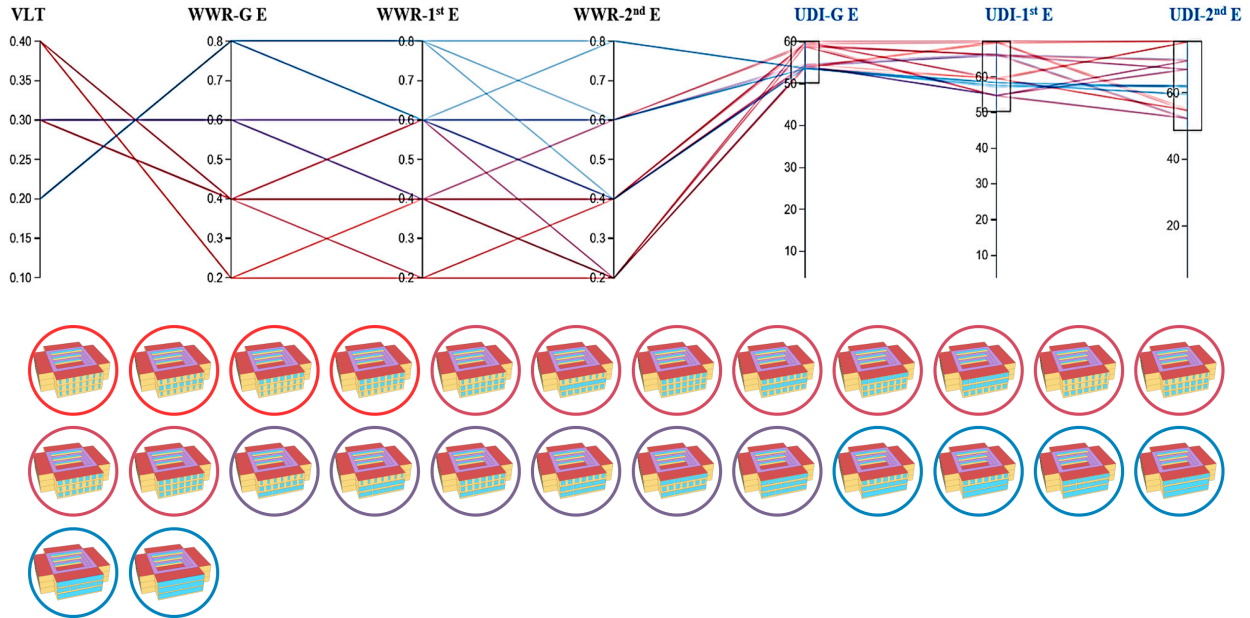

Figure 12. The optimum WWR and VLT based on $UDI_{300lux-1000lux}$ in each eastern floor level for courtyard typology using SPD switchable glazing.
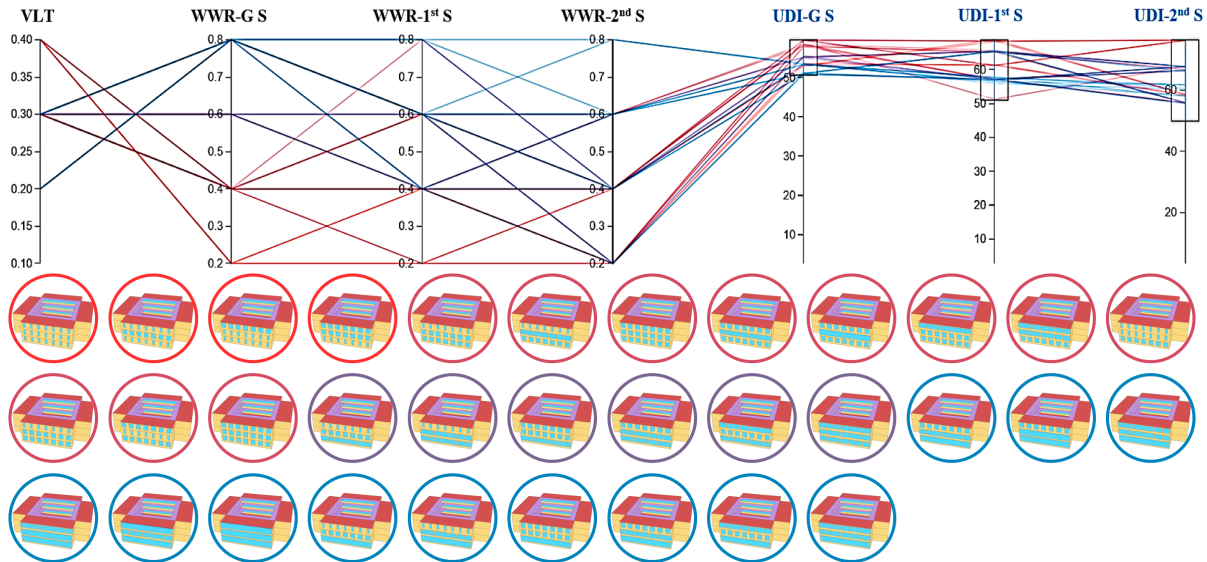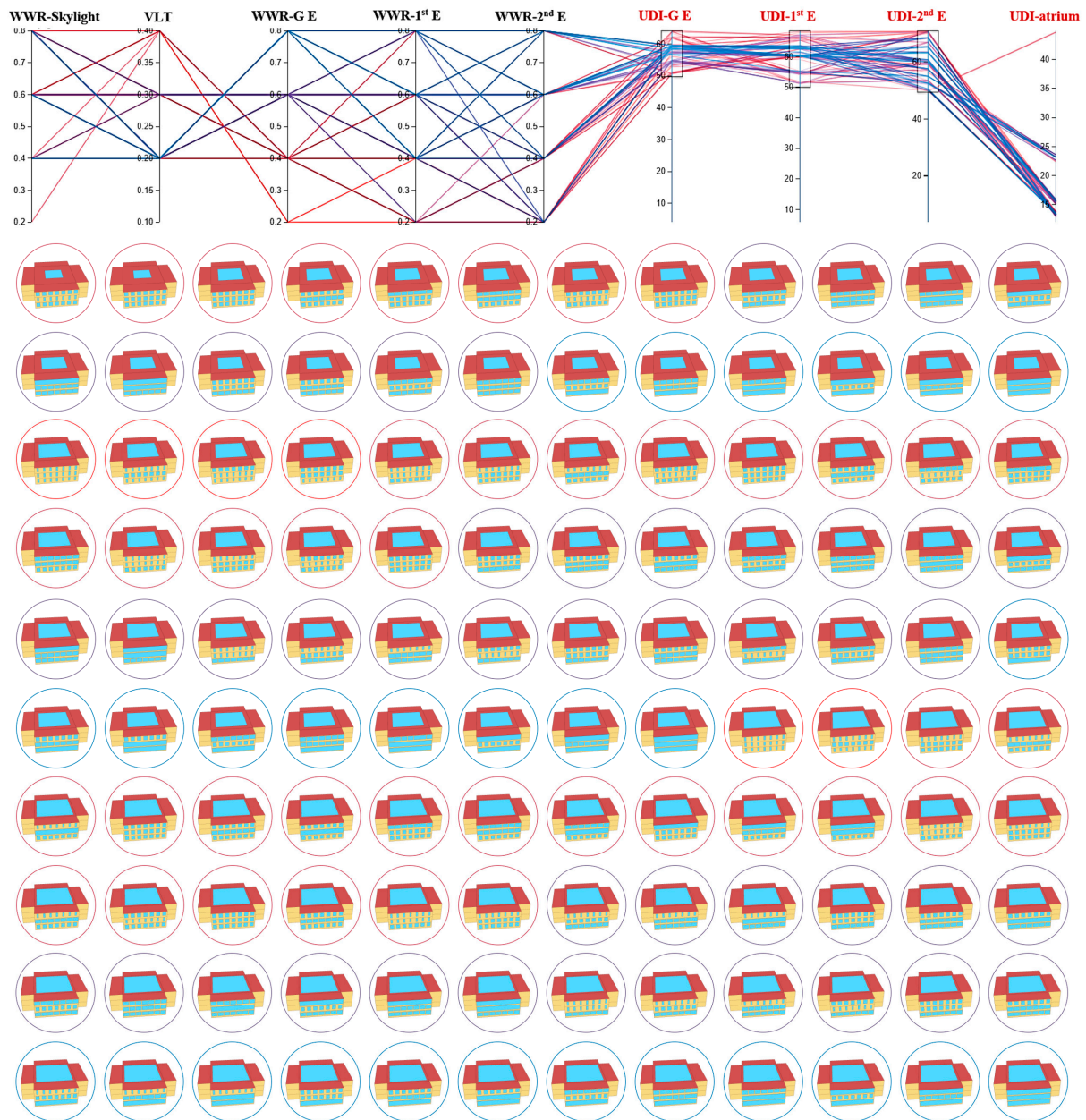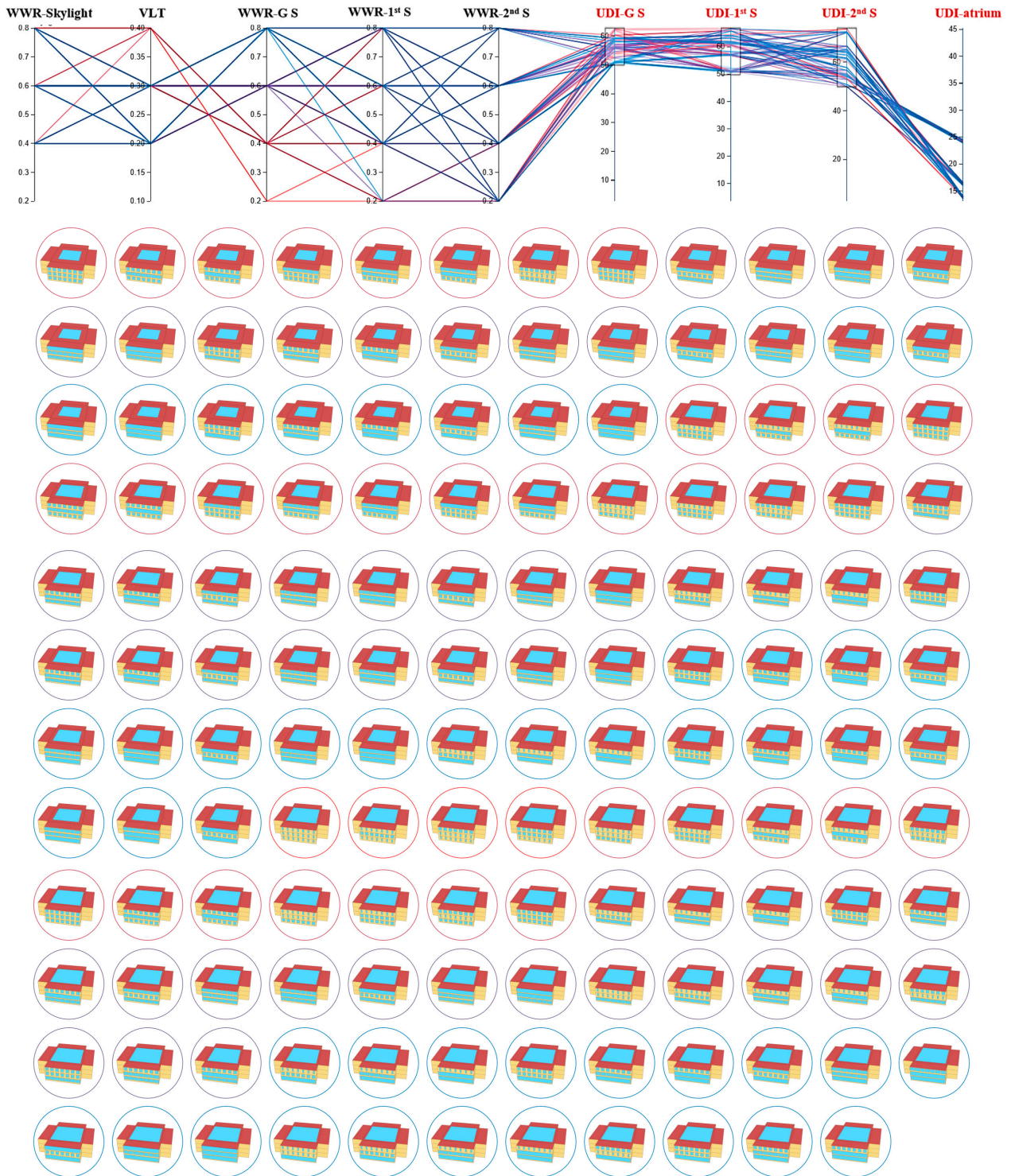

Figure 13. The optimum WWR and VLT based on $UDI_{300lux-1000lux}$ in each southern floor level for courtyard typology using SPD switchable glazing.

It is noteworthy that the illuminance levels in classrooms across different floors exhibited similar behavior, albeit with slight variations in $UDI_{300lux-1000lux}$ percentages. However, a counterproductive relationship was observed: a higher proportion of skylight ratio and SPD transmittance necessitated a lower WWR for external windows to achieve a balanced bilateral lighting mode and vice versa. However, the only two configurations that provided a significant $UDI_{300lux-1000lux}$ percentage in the atrium space involved a 20% skylight ratio in transparent SPD state, combined with either a 40% WWR across all floors or a 20% WWR on the first floor.

Figure 14. The optimum WWR and VLT based on $UDI_{300lux–1000lux}$ in each eastern floor level for atrium typology using SPD switchable glazing.

In the atrium typology, a larger skylight ratio was found to yield a better $UDI_{300lux–1000lux}$ percentage. Additionally, an alternative configuration considered a medium skylight ratio in combination with an intermediate SPD state. However, in southern classrooms on each level, a large WWR of 80% could be incorporated, while eastern classrooms were only combined with small and medium WWR options.

However, by integrating SPD technology in the atrium with clerestory school typology, a $UDI_{300lux–1000lux}$ exceeding 50% can be achieved through various configurations, specifically from 13 to 7 out of a total of 256 configurations for the east and south classrooms, respectively. The utilization of SPD intermediate1 (20%VLT) proves to be successful in achieving acceptable $UDI_{300lux–1000lux}$ levels when employing a large SPD glazed area (80%WWR) across all floors, with slight adjustments needed for the classrooms on the second floor due to direct sunlight ingress through the clerestory windows during working hours. Alternatively, the intermediate 2 setting (30%VLT) presents itself as a viable alternative configuration for schools with a 60%WWR. Notably, the optimal scenario within

this typology occurs when the SPD is in its transparent state, coupled with a 40%WWR. This configuration yields the highest $UDI_{300lux–1000lux}$ percentage, reaching up to 46% in the eastern and southern classrooms, especially within the atrium space, as depicted in Figures 16 and 17. This outcome signifies the superior performance of this typology compared to others investigated in this study.

Figure 15. The optimum WWR and VLT based on $UDI_{300lux–1000lux}$ in each southern floor level for atrium typology using SPD switchable glazing.
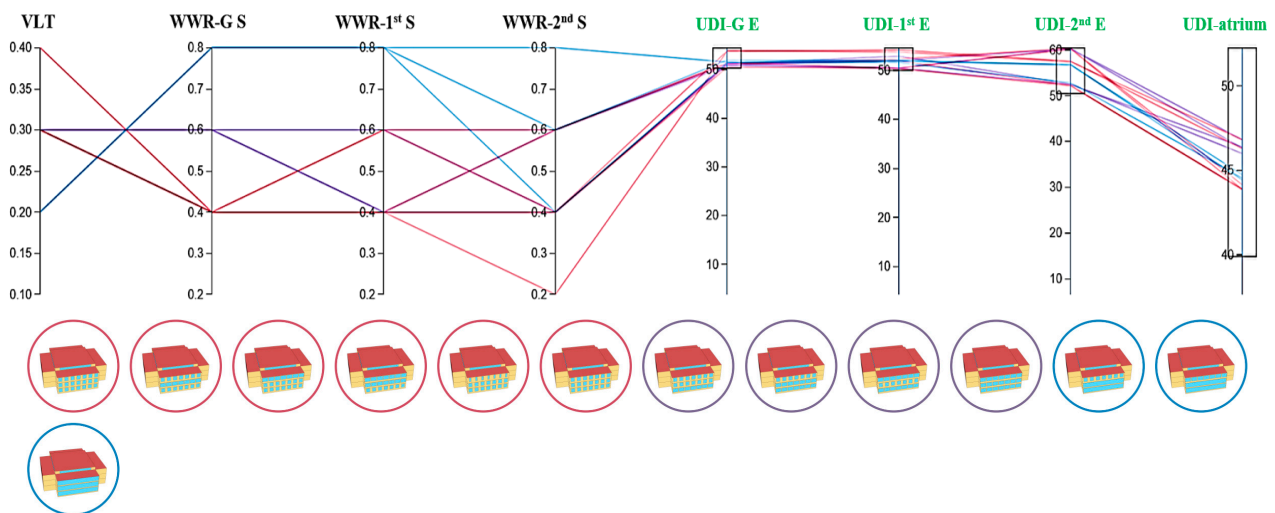
Figure 16. The optimum WWR and VLT based on UDI$_{300lux-1000lux}$ in each eastern floor level for clerestory typology using SPD switchable glazing.
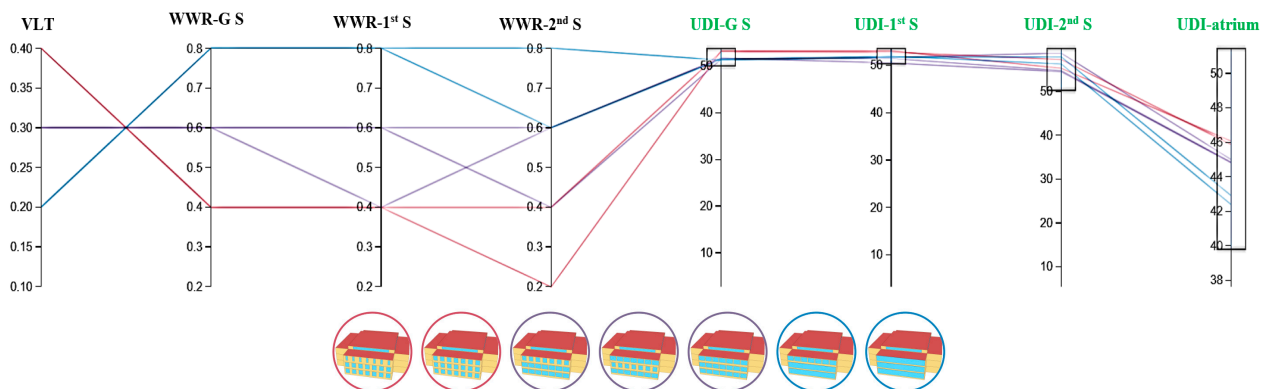
Figure 17. The optimum WWR and VLT based on UDI$_{300lux-1000lux}$ in each southern floor level for clerestory typology using SPD switchable glazing.

3.4. Comparison against SPD Glazing

Figure 18 presents a comprehensive comparative evaluation of the UDI$_{300lux-1000lux}$ metric, examining the utilization of SPD switchable glass in different architectural typologies (courtyard, atrium, clerestory) within various levels (ground, first, second) and orientations (south, east) in school settings.

- The courtyard design exhibits an intriguing pattern across levels. In the reference case and when employing SPD at 40% with a WWR of 20%, the UDI$_{300lux-1000lux}$ bin decreases as one ascends from the ground to the second level. However, this trend is reversed when the SPD is set at 40% VLT (Visible Light Transmission) with a WWR of 40%. In this case, an increase in UDI$_{300lux-1000lux}$ is observed as the levels progress, suggesting improved daylighting at higher levels. The annual improvement percentages range from 43% to 49% in southern and eastern classrooms on the upper levels, respectively.
- Similarly, the atrium with skylight design also demonstrates an increasing trend in UDI$_{300lux-1000lux}$ with each level, considering the specified settings. The highest UDI$_{300lux-1000lux}$ value (72% to 70%) is observed on the second level when utilizing SPD at 30% and a WWR of 40%. This indicates enhanced daylight penetration at higher levels, with improvements of up to 20% in southern classrooms and 16.9% in eastern classrooms.

- Conversely, the atrium with clerestory design exhibits a negative improvement in $UDI_{300lux-1000lux}$ with each level, considering the given settings. Despite integrating SPD switchable glazing in all states within the classrooms, the reference model still outperforms in terms of $UDI_{300lux-1000lux}$, albeit by a marginal margin not exceeding 4%. This discrepancy can be attributed to the limited illuminance entering from the top area and the low transmittance of the SPD glass employed in the external façade of the classrooms.
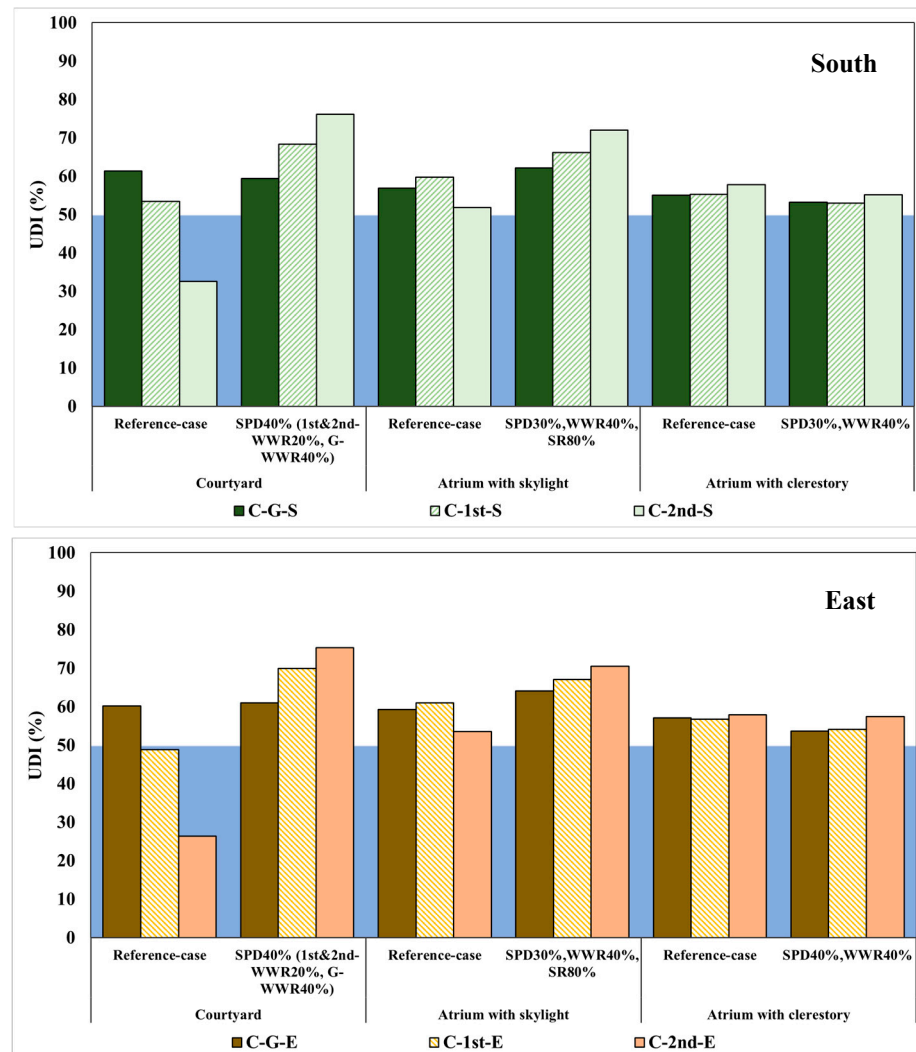
Figure 18. Comparison of $UDI_{300lux-1000lux}$ between reference and optimum models using the SPD transparency states and WWR of external glazing and skylight ratio.

3.5. Daylight Glare Probability (DGP) Analysis

Table 3 presents the impact of different school typologies and design configurations on glare potential in the eastern and southern classrooms at 9.00 a.m and 12.00 p.m, respectively, on the second floor at solstice summer and winter. The reference model exhibits perceptible glare during bo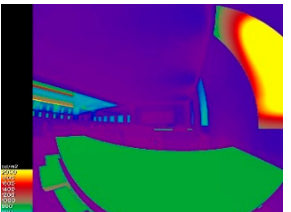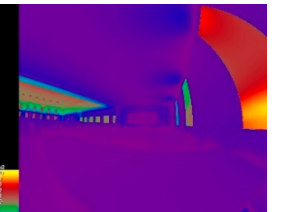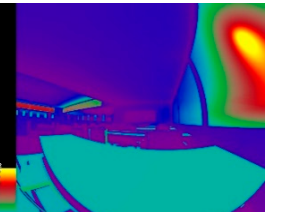th the winter and summer solstices. However, the optimum models, which incorporate the optimum SPD switchable glass transmittance state and varied WWRs, significantly improve glare control, as displayed in Figure 15. In the courtyard typology, the intolerable glare observed in the reference model is substantially reduced during the winter solstice, but not sufficient to overcome the issue of discomfort glare. The atrium typology achieves imperceptible glare levels in both solstices, while the clerestory typology shows a remarkable reduction in glare in particular at solstice summer.

Table 3. Daylight glare probability of various typologies schools against the optimum design proposed using SPD smart glass.

Typologies		Courtyard		Atrium with Skylight		Atrium with Clerestory	
	Time	Solstice Winter	Solstice Summer	Solstice Winter	Solstice Summer	Solstice Winter	Solstice Summer
Eastern Classrooms	Reference model						
	DGP	Intolerable 1	Perceptible 0.35	Perceptible 0.35	Imperceptible 0.22	Imperceptible 0.24	Perceptible 0.36
	Optimum model						
	DGP	Intolerable 0.75	Imperceptible 0.25	Imperceptible 0.21	Imperceptible 0.13	Intolerable 0.21	Imperceptible 0.25
Southern Classrooms	Reference model						
	DGP	Perceptible 0.35	Imperceptible 0.23	Perceptible 0.36	Imperceptible 0.22	Perceptible 0.37	Imperceptible 0.23
	Optimum model						
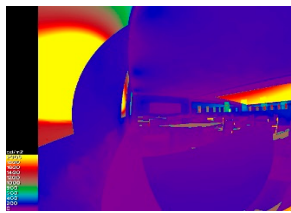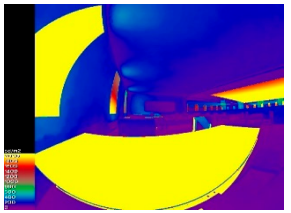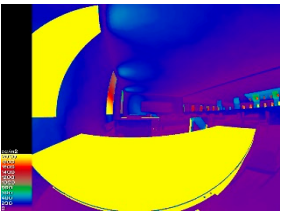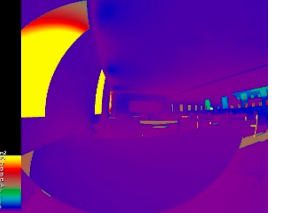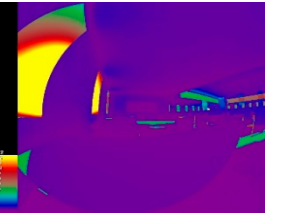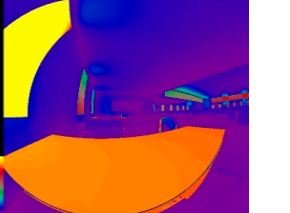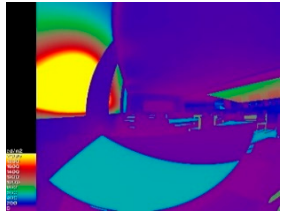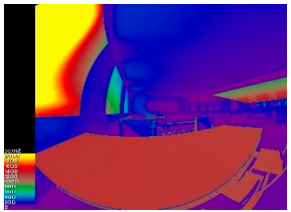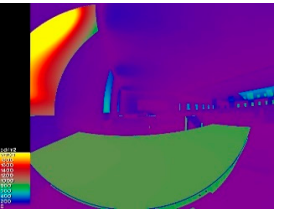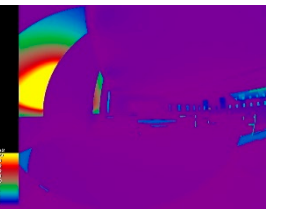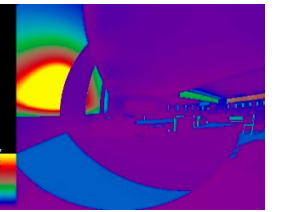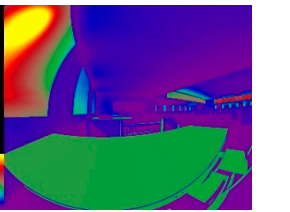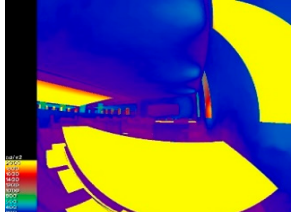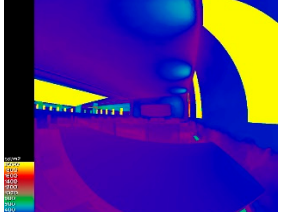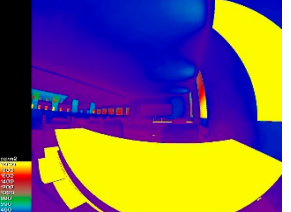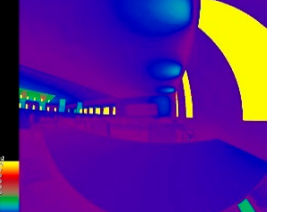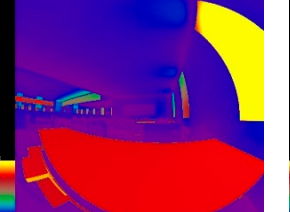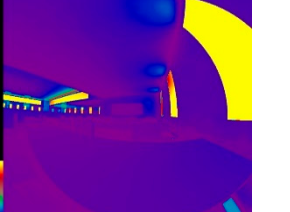
On the other hand, the analysis of DGP in the southern classrooms for reference model exhibits perceptible glare during the winter solstice, while the summer solstice demonstrates an imperceptible glare level. However, the proposed optimum models, incorporating SPD switchable glass and the optimum of the WWRs, effectively mitigate glare issues. The DGP values for all typologies and solstices remain imperceptible, emphasizing the successful reduction of glare discomfort. These results demonstrate the significance of utilizing SPD switchable glass and optimizing the WWRs to create a comfortable and visually pleasant learning environment in southern classrooms.
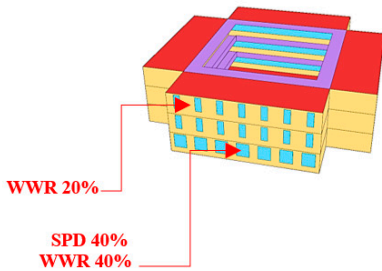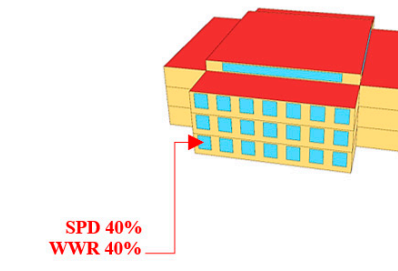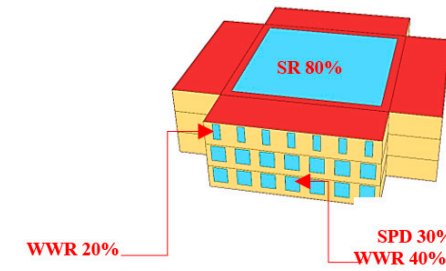
4. Discussion

The daylighting analysis in different architectural schools' typologies, including courtyards and atriums, revealed significant insights into how design elements influence illuminance distribution and visual comfort. The study found that eastern façades in courtyard typologies exhibited higher illuminance levels in the morning during summer solstice, while northern façades experienced extreme illuminance during winter noon. This variation highlights the importance of orientation and floor level in daylighting strategies, confirming previous research by Alwetaishi et al., which emphasized the need for optimized WWR and orientation based on climatic conditions. In atrium typologies, internal architectural features like skylights and internal windows played a crucial role in daylight penetration, supporting Ma and Yang's findings [34] on the optimal design parameters for atrium daylighting performance. The high UDI and sDA values in atrium configurations indicated sufficient daylight availability throughout the year, but excessive brightness and glare necessitated advanced shading solutions, consistent with studies by Xue and Liu [38] and Mesloub et al. [28] on managing daylight quality and glare through strategic design and smart glazing systems.

Furthermore, incorporating adjustable shading devices, such as automated blinds and louvers, alongside SPD switchable glazing is essential for achieving optimal daylighting. These dynamic shading solutions effectively control brightness and glare by adjusting to real-time lighting conditions, enhancing visual comfort. Research by Fang and Cho supports the efficacy of these systems in managing glare and improving daylight quality. This holistic approach, combining advanced glazing with adaptive shading, is crucial for creating visually comfortable and energy-efficient educational environments.

The integration of SPD switchable glazing systems demonstrated substantial improvements in daylighting performance, particularly when using intermediate transparency states (30% VLT) combined with appropriate WWRs, as shown in figures in Table 4. These configurations effectively balanced daylight levels and glare control, resonating with Potočnik and Košir's [45] research on the importance of WWR and glazing transmissivity. Higher skylight ratios, in conjunction with SPD glazing, significantly enhanced UDI values in atrium typologies, illustrating the synergy between skylight design and daylight performance, as highlighted by Ferreira et al. [41] The DGP analysis further confirmed the efficacy of optimized SPD glazing in reducing glare, especially in atrium and clerestory typologies during solstices, aligning with Fang and Cho's findings [44] on the impact of skylight dimensions on glare control. These results underscore the critical role of adaptive glazing technologies and strategic design interventions in creating visually comfortable and energy-efficient educational environments.

Table 4. Optimum SPD switchable glazing system integrated into main schools' typologies.

Optimum SPD Integration with Courtyard Typology	Optimum SPD Integration with Atrium with Clerestory Typology	Optimum SPD Integration with Skylight Typology
WWR 20% SPD 40% WWR 40%	SPD 40% WWR 40%	SR 80% WWR 20% SPD 30% WWR 40%

5. Conclusions

The current study highlights the significance of analyzing different typologies of schools to enhance visual comfort. Specifically, this research introduces a novel approach by integrating SPD smart switchable glazing systems into three school typologies: courtyard, atrium with skylight or clerestory. Furthermore, an optimization technique is proposed, which utilizes the $UDI_{300lux-1000lux}$ and DGP metrics through parametric analysis, considering various variables such as orientation, floor levels, WWR of external glazing, transmittance states of SPD, and skylight ratio for atrium typology. An extensive radiance simulation was conducted using honeybee and ladybug plugins for rhino 7 software to conduct a comprehensive evaluation. This methodology provided detailed insights into the changes in illuminance and uniformity at different floor levels of the working plane on an hourly basis throughout the year. Based on the findings, the following conclusions can be drawn:

1. Firstly, the atrium with a clerestory design exhibits a negative impact on $UDI_{300lux-1000lux}$ with each level when compared to the reference model. On the other hand, the courtyard and atrium designs demonstrate an increasing trend in $UDI_{300lux-1000lux}$ across all levels, particularly at higher levels.

2. Secondly, the integration of optimized SPD switchable glass transmittance states and appropriate WWRs significantly enhances glare control, thereby creating a comfortable and visually pleasant learning environment in southern classrooms.

3. Finally, the study proposes the following optimum design configurations for each school typology and orientation, utilizing SPD switchable glass:

   - *Courtyard typology:* Transparent SPD state (40%) with 40% WWR on the ground floor and 20% WWR on the upper floors.
   - *Atrium with skylight typology:* Intermediate SPD state (30%) with 40% WWR and a large skylight ratio of 80%.
   - *Atrium with clerestory typology:* Transparent SPD state (40%) with 40% WWR on all floors.

Despite the valuable insights provided by this study, several limitations should be acknowledged. Firstly, the study focuses on school typologies specific to Saudi Arabia, adhering to the local authorities' time schedules and regulatory frameworks. This study did not consider some factors influencing the visual comfort of the SPD smart glazing system, such as the color rendering index and color temperature. Future research should address these limitations by incorporating real-world case studies to validate the simulation results. Additionally, examining the energetic and thermal performance of SPD systems in various climatic conditions would enhance the generalizability of the findings. Further studies should also investigate the economic feasibility and long-term benefits of SPD systems in school environments. Moreover, exploring the integration of SPD glazing with other sustainable building technologies could provide a more comprehensive approach to improving visual comfort and energy efficiency in educational buildings. In the end,

these findings contribute to the understanding and improvement of visual comfort in school environments. The integration of SPD switchable glazing systems, coupled with the suggested design configurations, can provide valuable guidance for architects and designers in creating optimal learning spaces that prioritize visual comfort and well-being.

Author Contributions: A.M.: writing original manuscript, conceptualization, formal analysis, method, software; M.M.A.: writing review editing, resources, visualization; G.A.: writing review editing, conceptualization; K.E.: data curation, investigation; R.H.: writing review editing, formal analysis; A.G.: writing review editing, conceptualization, method; M.S.M.: writing review editing, visualization. All authors have read and agreed to the published version of the manuscript.

Data Availability Statement: The data supporting the findings of this study are available from the corresponding author upon request.

Conflicts of Interest: The authors declare no conflict of interest.

Nomenclature

SPD	suspended particle devices
WWR	Window-to-Wall Ratios
SR	Skylight Ratios
WPI	Work plane illuminance
Ui	uniformity index
IEQ	Indoor environmental quality
EPA	Environmental Protection Agency
PDLC	polymer-dispersed liquid crystal
EC	electrochromic
AC	Alternative current
PV	Photovoltaic
UDI	Useful Daylight Illuminance
DGP	Daylight Glare Probability
sDA	Spatial Daylight autonomy
G.F	Ground floor
1st.F/2nd F	First/second floor
VLT	Visible light Transmittance
BSDF	Bidirectional Scattering Distribution Function

References

1. Vilcekova, S.; Meciarova, L.; Burdova, E.K.; Katunska, J.; Kosicanova, D.; Doroudiani, S. Indoor environmental quality of classrooms and occupants' comfort in a special education school in Slovak Republic. *Build. Environ.* **2017**, *120*, 29–40. [CrossRef]
2. Almeida, R.M.; De Freitas, V.P. Indoor environmental quality of classrooms in Southern European climate. *Energy Build.* **2014**, *81*, 127–140. [CrossRef]
3. Choi, S.; Guerin, D.A.; Kim, H.-Y.; Brigham, J.K.; Bauer, T. Indoor Environmental Quality of Classrooms and Student Outcomes: A Path Analysis Approach. *J. Learn. Spaces* **2014**, *2*, 2013–2014.
4. Turunen, M.; Toyinbo, O.; Putus, T.; Nevalainen, A.; Shaughnessy, R.; Haverinen-Shaughnessy, U. Indoor environmental quality in school buildings, and the health and wellbeing of students. *Int. J. Hyg. Environ. Health* **2014**, *217*, 733–739. [CrossRef]
5. Haverinen-Shaughnessy, U.; Shaughnessy, R.J.; Cole, E.C.; Toyinbo, O.; Moschandreas, D.J. An assessment of indoor environmental quality in schools and its association with health and performance. *Build. Environ.* **2015**, *93*, 35–40. [CrossRef]
6. Young, B.N.; Benka-Coker, W.O.; Weller, Z.D.; Oliver, S.; Schaeffer, J.W.; Magzamen, S. How does absenteeism impact the link between school's indoor environmental quality and student performance? *Build. Environ.* **2021**, *203*, 108053. [CrossRef]
7. Benka-Coker, W.; Young, B.; Oliver, S.; Schaeffer, J.W.; Manning, D.; Suter, J.; Cross, J.; Magzamen, S. Sociodemographic variations in the association between indoor environmental quality in school buildings and student performance. *Build. Environ.* **2021**, *206*, 108390. [CrossRef]

8. De Luca, F.; Sepúlveda, A.; Varjas, T. Multi-performance optimization of static shading devices for glare, daylight, view and energy consideration. *Build. Environ.* **2022**, *217*, 109110. [CrossRef]

9. Lee, S.; Lee, K.S. A Study on the improvement of the evaluation scale of discomfort glare in educational facilities. *Energies* **2019**, *12*, 3265. [CrossRef]

10. Hamedani, Z.; Solgi, E.; Hine, T.; Skates, H.; Isoardi, G.; Fernando, R. Lighting for work: A study of the relationships among discomfort glare, physiological responses and visual performance. *Build. Environ.* **2020**, *167*, 106478. [CrossRef]

11. Fakhari, M.; Vahabi, V.; Fayaz, R. A study on the factors simultaneously affecting visual comfort in classrooms: A structural equation modeling approach. *Energy Build.* **2021**, *249*, 111232. [CrossRef]

12. Ali, M.M.; Al-Kodmany, K.; Armstrong, P.J. Energy Efficiency of Tall Buildings: A Global Snapshot of Innovative Design. *Energies* **2023**, *16*, 2063. [CrossRef]

13. Toodekharman, H.; Abravesh, M.; Heidari, S. Visual Comfort Assessment of Hospital Patient Rooms with Climate Responsive Facades. *J. Daylighting* **2023**, *10*, 17–30. [CrossRef]

14. Mohammad, A.K.; Ghosh, A. Exploring energy consumption for less energy-hungry building in UK using advanced aerogel window. *Sol. Energy* **2023**, *253*, 389–400. [CrossRef]

15. Zhou, Y.; Ma, M.; Tam, V.W.; Le, K.N. Design variables affecting the environmental impacts of buildings: A critical review. *J. Clean. Prod.* **2023**, *387*, 135921. [CrossRef]

16. Alwetaishi, M.; Taki, A. Investigation into energy performance of a school building in a hot climate: Optimum of window-to-wall ratio. *Indoor Built Environ.* **2020**, *29*, 24–39. [CrossRef]

17. Temiz, M.; Dincer, I. Design and assessment of a solar energy based integrated system with hydrogen production and storage for sustainable buildings. *Int. J. Hydrogen Energy* **2023**, *48*, 15817–15830. [CrossRef]

18. Asfour, O.S. A comparison between the daylighting and energy performance of courtyard and atrium buildings considering the hot climate of Saudi Arabia. *J. Build. Eng.* **2020**, *30*, 101299. [CrossRef]

19. Pinto, M.C.; Crespi, G.; Dell'Anna, F.; Becchio, C. Combining energy dynamic simulation and multi-criteria analysis for supporting investment decisions on smart shading devices in office buildings. *Appl. Energy* **2023**, *332*, 120470. [CrossRef]

20. Do, C.T.; Chan, Y.-C.; Phuong, N.T.K. Selection of spatial sensitivity curve and installation location of photosensors for daylight-linked control systems in space with dynamic shading devices. *Build. Environ.* **2023**, *230*, 109984. [CrossRef]

21. Ghosh, A. Investigation of vacuum-integrated switchable polymer dispersed liquid crystal glazing for smart window application for less energy-hungry building. *Energy* **2023**, *265*, 126396. [CrossRef]

22. Piccolo, A.; Prestipino, M.; Panzera, M.F.; Baccoli, R. Study of the Correlation among Luminous Properties of Smart Glazing for Adaptive Energy Saving Buildings. *Buildings* **2023**, *13*, 337. [CrossRef]

23. Ji, Y.; Xu, M.; Zhang, T.; He, Y. Intelligent Parametric Optimization of Building Atrium Design: A Case Study for a Sustainable and Comfortable Environment. *Sustainability* **2023**, *15*, 4362. [CrossRef]

24. Marzouk, M.; ElSharkawy, M.; Mahmoud, A. Optimizing daylight utilization of flat skylights in heritage buildings. *J. Adv. Res.* **2022**, *37*, 133–145. [CrossRef]

25. Ibrahim, Y.; Kershaw, T.; Shepherd, P.; Elkady, H. Multi-objective optimisation of urban courtyard blocks in hot arid zones. *Sol. Energy* **2022**, *240*, 104–120. [CrossRef]

26. Mesloub, A.; Ghosh, A.; Kolsi, L.; Alshenaifi, M. Polymer-Dispersed Liquid Crystal (PDLC) smart switchable windows for less-energy hungry buildings and visual comfort in hot desert climate. *J. Build. Eng.* **2022**, *59*, 105101. [CrossRef]

27. Oh, M.; Jang, M.; Moon, J.; Roh, S. Evaluation of building energy and daylight performance of electrochromic glazing for optimal control in three different climate zones. *Sustainability* **2019**, *11*, 287. [CrossRef]

28. Mesloub, A.; Ghosh, A.; Touahmia, M.; Albaqawy, G.A.; Alsolami, B.M.; Ahriz, A. Assessment of the overall energy performance of an SPD smart window in a hot desert climate. *Energy* **2022**, *252*, 124073. [CrossRef]

29. Ghosh, A.; Norton, B.; Duffy, A. Daylighting performance and glare calculation of a suspended particle device switchable glazing. *Sol. Energy* **2016**, *132*, 114–128. [CrossRef]

30. Ghosh, A.; Norton, B.; Duffy, A. Measured thermal performance of a combined suspended particle switchable device evacuated glazing. *Appl. Energy* **2016**, *169*, 469–480. [CrossRef]

31. Nundy, S.; Ghosh, A. Thermal and visual comfort analysis of adaptive vacuum integrated switchable suspended particle device window for temperate climate. *Renew. Energy* **2020**, *156*, 1361–1372. [CrossRef]

32. Ghosh, A.; Norton, B. Optimization of PV powered SPD switchable glazing to minimise probability of loss of power supply. *Renew. Energy* **2019**, *131*, 993–1001. [CrossRef]

33. Paradise World Buildsquare Private Limited. White Double Glazed Window. 2024. Available online: https://www.indiamart.com/proddetail/double-glazed-window-16185768533.html (accessed on 10 June 2024).

34. Ma, J.; Yang, Q. Optimizing Annual Daylighting Performance for Atrium-Based Classrooms of Primary and Secondary Schools in Nanjing, China. *Buildings* **2022**, *13*, 11. [CrossRef]

35. Marzouk, M.; ElSharkawy, M.; Eissa, A. Optimizing thermal and visual efficiency using parametric configuration of skylights in heritage buildings. *J. Build. Eng.* **2020**, *31*, 101385. [CrossRef]

36. Mohelnikova, J.; Hirs, J. Effect of externally and internally reflective components on interior daylighting. *J. Build. Eng.* **2016**, *7*, 31–37. [CrossRef]

37. Kaminska, A.; Ożadowicz, A. Lighting control including daylight and energy efficiency improvements analysis. *Energies* **2018**, *11*, 2166. [CrossRef]

38. Xue, Y.; Liu, W. A Study on Parametric Design Method for Optimization of Daylight in Commercial Building's Atrium in Cold Regions. *Sustainability* **2022**, *14*, 7667. [CrossRef]

39. Talip, M.S.; Shaari, M.F.; Ahmad, S.S.; Sanchez, R.B. Optimising Daylighting Performance in Tropical Courtyard and Atrium Buildings for Occupants' Wellbeing. *Environ. Behav. Proc. J.* **2021**, *6*, 93–102. [CrossRef]

40. Wu, P.; Zhou, J.; Li, N. Influences of atrium geometry on the lighting and thermal environments in summer: CFD simulation based on-site measurements for validation. *Build. Environ.* **2021**, *197*, 107853. [CrossRef]

41. Ferreira, T.; Bournas, I.; Dubois, M.-C. Effect of atrium geometry and reflectance on daylighting in adjacent rooms. *J. Phys. Conf. Ser.* **2019**, *1343*, 012167. [CrossRef]

42. Ferreira, T. Daylight Optimization in an Office Building through Atrium Improvements. Master Thesis, Lund University, Lund, Sweden, 2018.

43. Yunus, J.; Ahmad, S.S.; Zain-Ahmed, A. Daylight performances of atrium buildings for different roof configuration under Malaysia sky conditions. *MATEC Web Conf.* **2019**, *266*, 01001. [CrossRef]

44. Fang, Y.; Cho, S. Design optimization of building geometry and fenestration for daylighting and energy performance. *Sol. Energy* **2019**, *191*, 7–18. [CrossRef]

45. Potočnik, J.; Košir, M. Influence of geometrical and optical building parameters on the circadian daylighting of an office. *J. Build. Eng.* **2021**, *42*, 102402. [CrossRef]

46. Medvedeva, N.; Kolesnikov, S. Specifics of Daylight in Atrium Spaces of Architectural Objects. *IOP Conf. Ser. Mater. Sci. Eng.* **2021**, *1079*, 022066. [CrossRef]

47. Acosta, I.; Varela, C.; Molina, J.F.; Navarro, J.; Sendra, J.J. Energy efficiency and lighting design in courtyards and atriums: A predictive method for daylight factors. *Appl. Energy* **2018**, *211*, 1216–1228. [CrossRef]

48. Wang, L.; Huang, Q.; Zhang, Q.; Xu, H.; Yuen, R.K. Role of atrium geometry in building energy consumption: The case of a fully air-conditioned enclosed atrium in cold climates, China. *Energy Build.* **2017**, *151*, 228–241. [CrossRef]

49. Vaisman, G.; Horvat, M. Influence of internal courtyards on the energy load and hours of illuminance in row houses in Toronto. *Energy Procedia* **2015**, *78*, 1799–1804. [CrossRef]

50. Reinhart, C.F.; Mardaljevic, J.; Rogers, Z. Dynamic daylight performance metrics for sustainable building design. *Leukos* **2006**, *3*, 7–31. [CrossRef]

51. Shemiranib, F.M.-S.M.M.; Tahbazc, M. Evaluation and Analysis of the Efficiency of Dynamic Metrics Evaluating Daylight Performance (Daylight Autonomy and Useful Daylight Illuminance) through Sensitivity Analysis; Case Study: Elementary Classroom in Tehran. *J. Archit. Urban Des. Urban Plan.* **2020**, *13*, 145–156.

52. D'Agostino, D.; D'Agostino, P.; Minelli, F.; Minichiello, F. Proposal of a new automated workflow for the computational performance-driven design optimization of building energy need and construction cost. *Energy Build.* **2021**, *239*, 110857. [CrossRef]